ChemBioChem

Supporting Information

The Total Synthesis of Glycolipids from *Streptococcus pneumoniae* and a Re-evaluation of Their Immunological Activity**

Seyed Iraj Sadraei, Greg Yousif, S. Maryamdokht Taimoory, Maryam Kosar, Samaneh Mehri, Raghd Alolabi, Emmanuel Igbokwe, Jason Toma, Mir Munir A. Rahim,* and John F. Trant*

1. Supplementary Figures

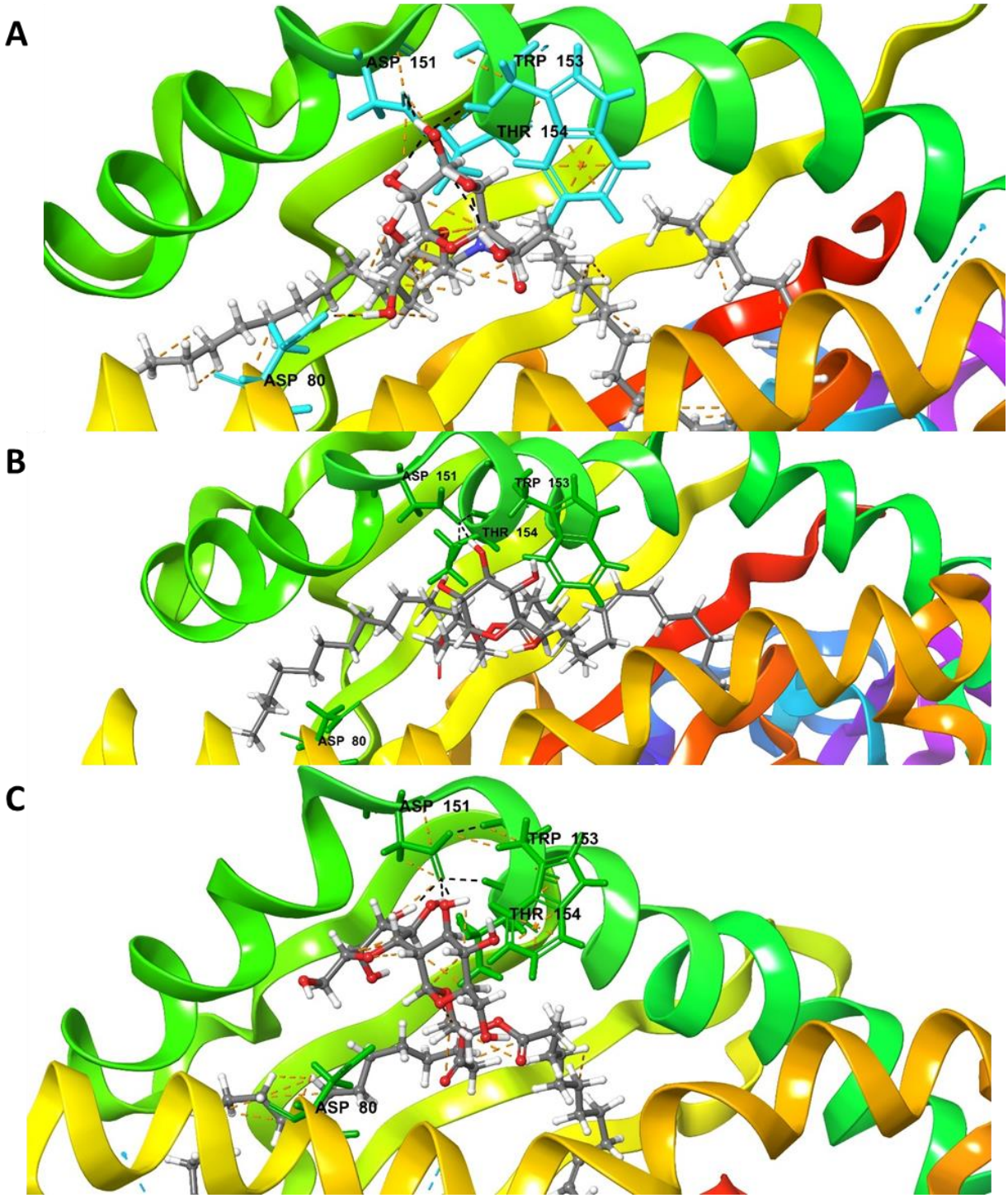

Figure S1. Highlighting key interactions at the mouth of the CD1d binding groove with A) KRN7000, B) Disaccharide **3**, and C) Monosaccharide **2**.

Docking Study:

To evaluate which pose best replicates the important interactions characteristic of the human CD1d with α-Galactosylceramide we reported both the S-score with the lowest value (the first series of docking posed that superimposed together; Figure S3) and the least value of RMSD (RMSD between the docked and the input structure). The lowest energetic values of both the "S score" and the "E_refine" as well as a low RMSD of conformer 1 is selected as the best pose and used for further MD simulation. The RMSD of above 2 Å reflects the significant differences between the different poses. The lowest energy pose is extremely similar to the X-ray crystal structure, although the carbohydrate adopts a slightly different pose when exposed to the water solvent.

	Conformer 1	**Conformer 2**
S score	-16.0875	-14.6502
E_refine	-55.6458	-45.2061
RMSD	2.0928	3.0557

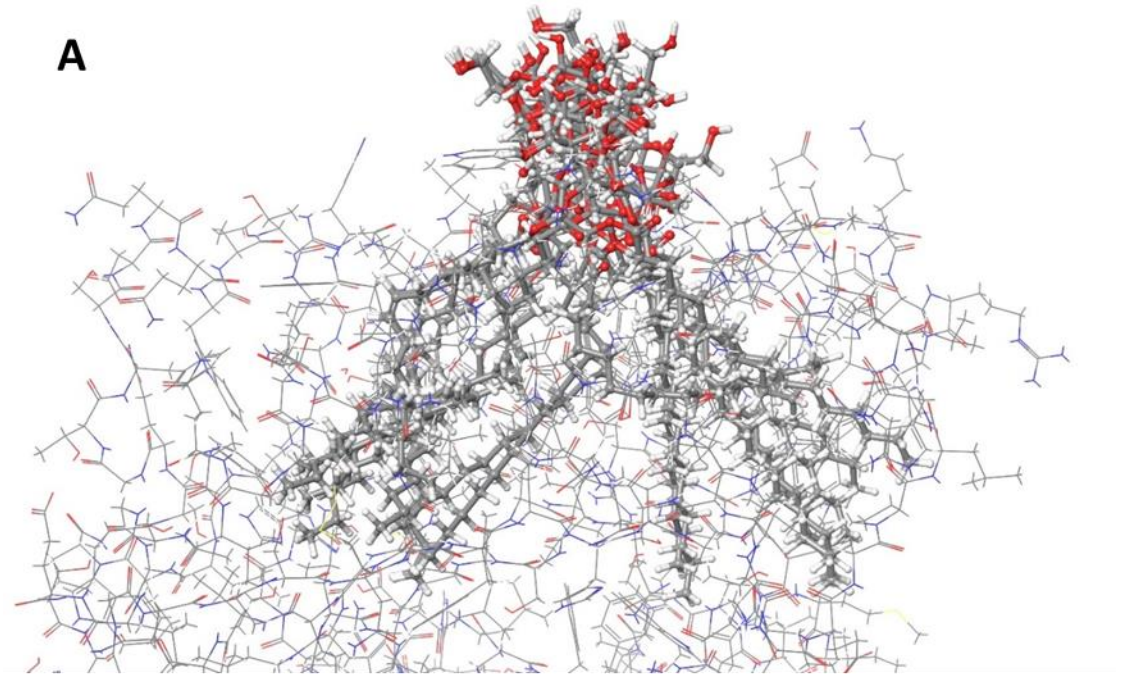

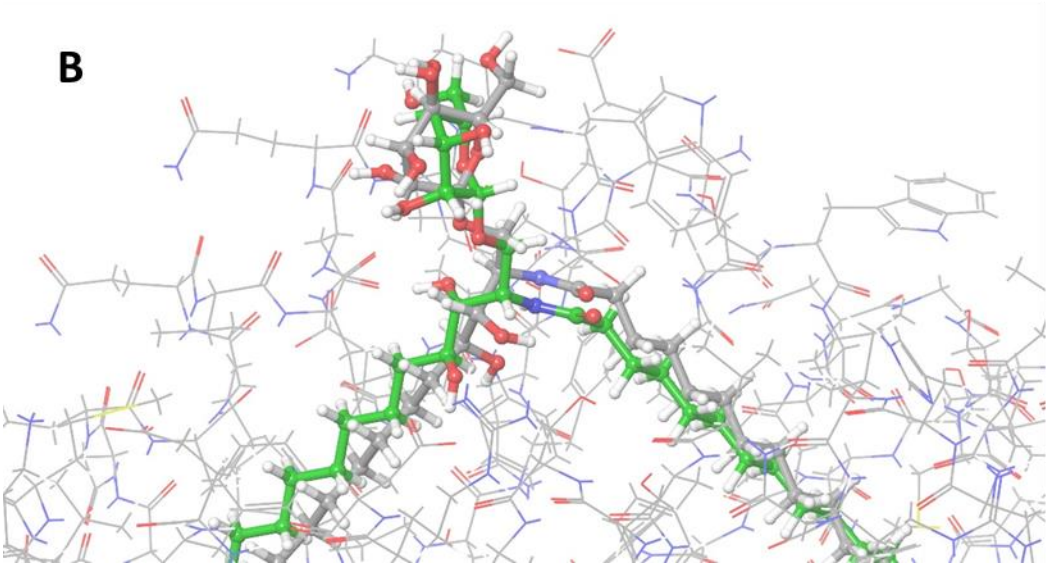

Figure S2. A) The superimposed binary structure of diverse docking poses obtained from rigid docking results for KRN7000 (1ZT4; The crystal structure of human CD1d with α-Galactosylceramide). These structures obtained are comparable to those in the crystal structure. The lowest energy docked structure is essentially identical with the crystal structure of the dimeric complex; **B)** The crystal structure of KRN7000 (green) superimposed with the optimal docked structure (grey).

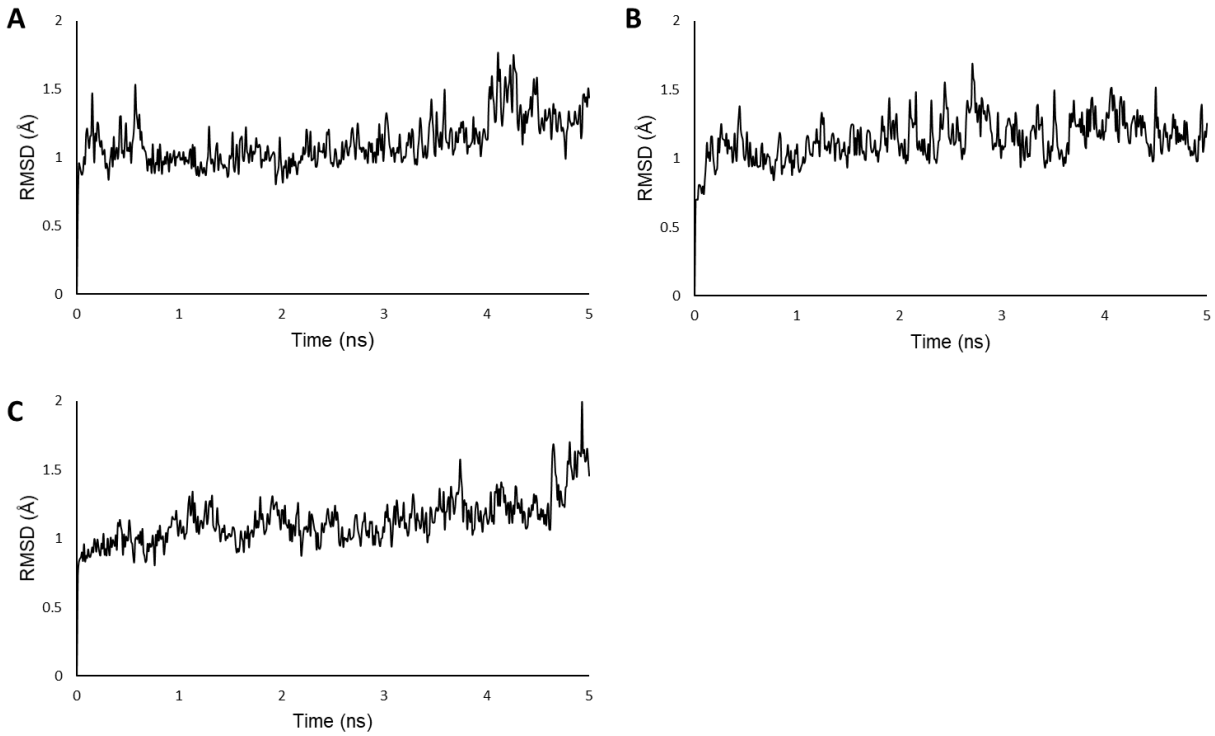

Figure S3. RMSD plot representing the complex of human CD1d bound to A) **KRN7000**; B) monosaccharide **2**; and C) disaccharide **3**.

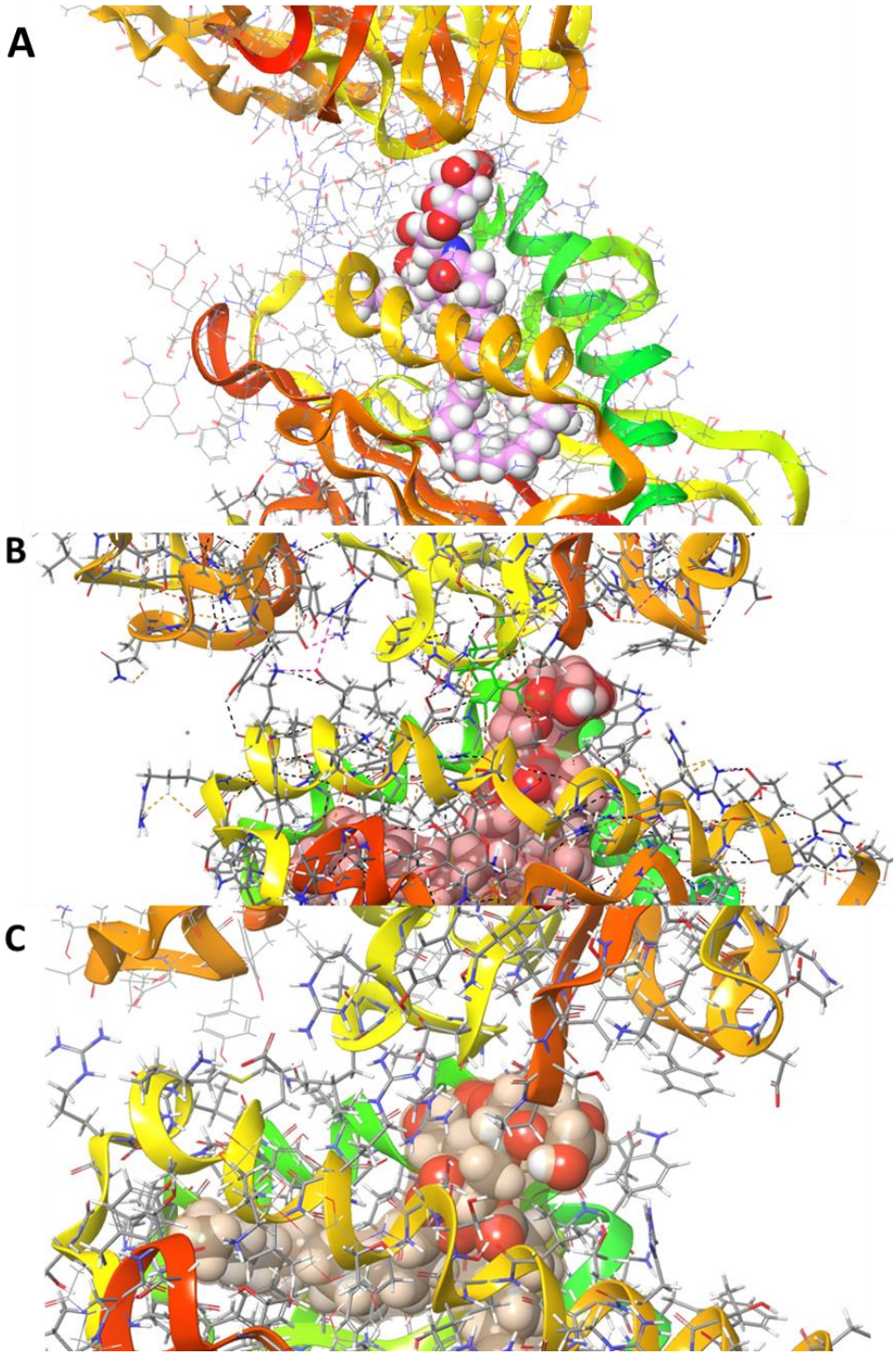

Figure S4. Visualization of the modelled ternary complex highlighting differences in key interactions. Structure is obtained from the energy minimum conformation from the MD simulation (extracted from the 5 ns NPT). A) **TCR∩KRN7000@CD1d**; B) **TCR∩2@CD1d** ;C) **TCR∩3@CD1d**

.

2. Spectra of New Compounds

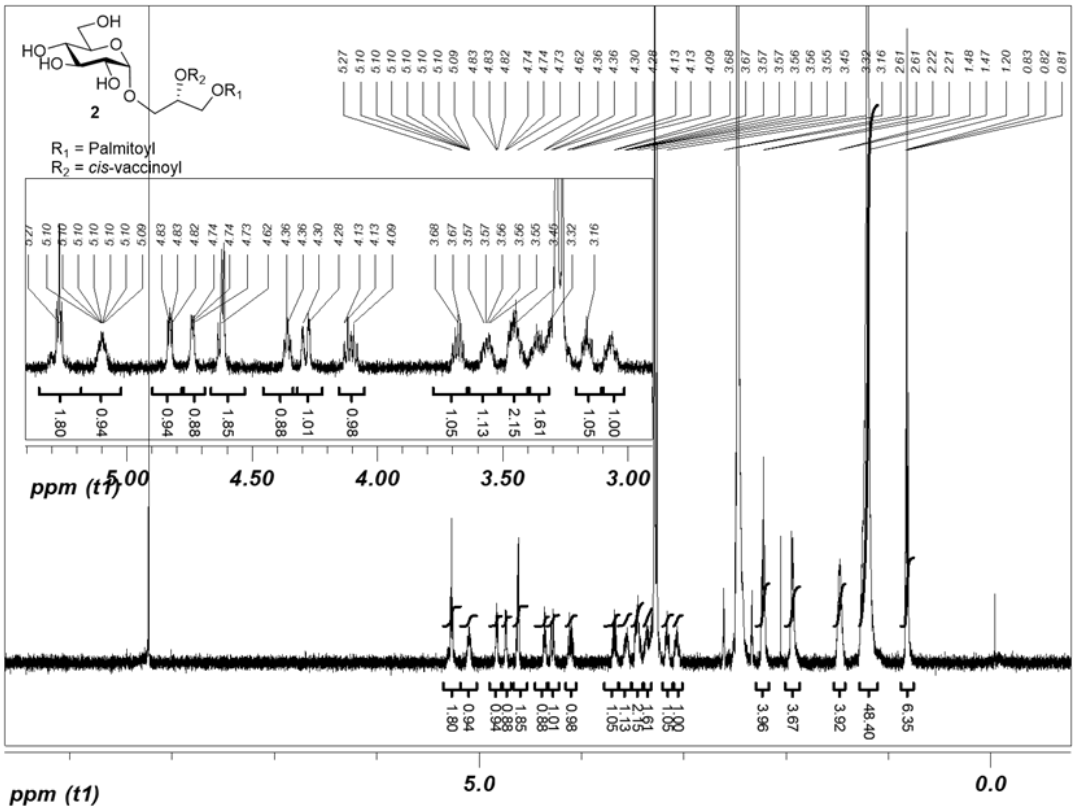

Figure S5. ^{1}H NMR (500 MHz d_6-Me_2SO-$CDCl_3$ (5:1, v/v) of compound 2. Spectrum is superimposable with that provided in Kinjo et al.[1]

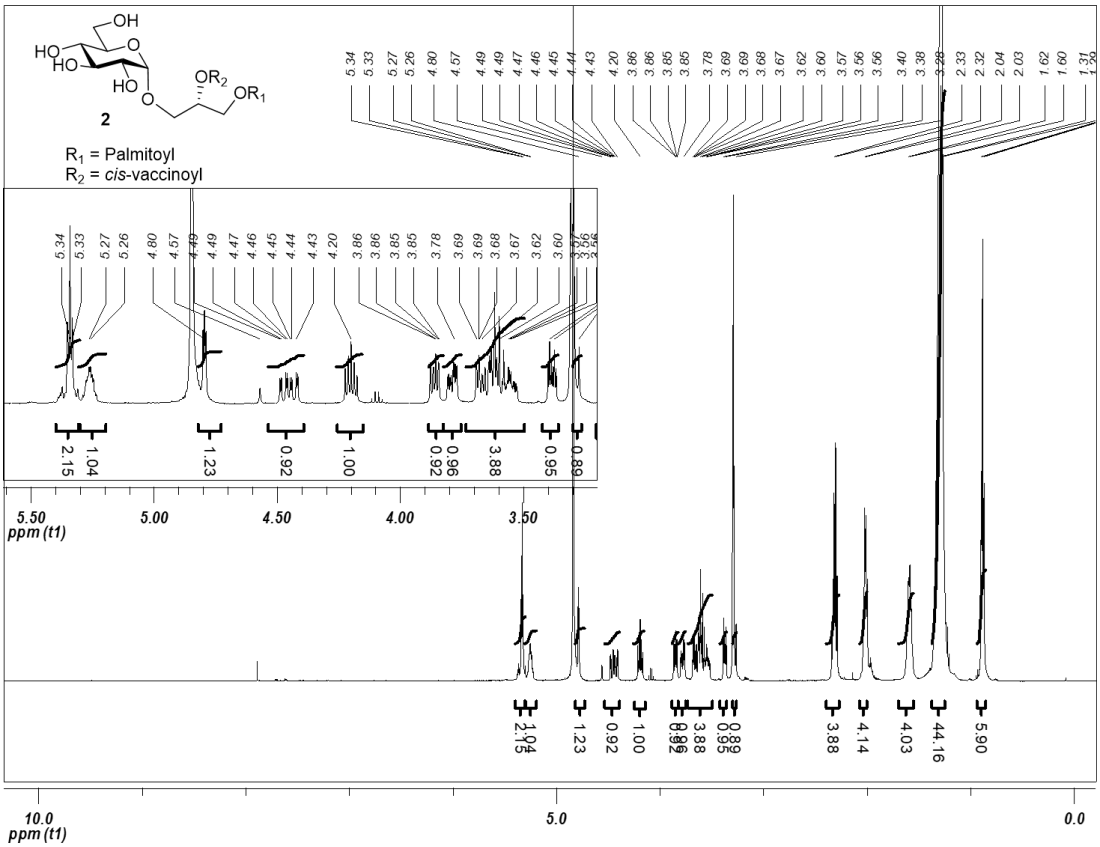

Figure S6. ^{1}H NMR (500MHz, MeOD) of compound **2**.

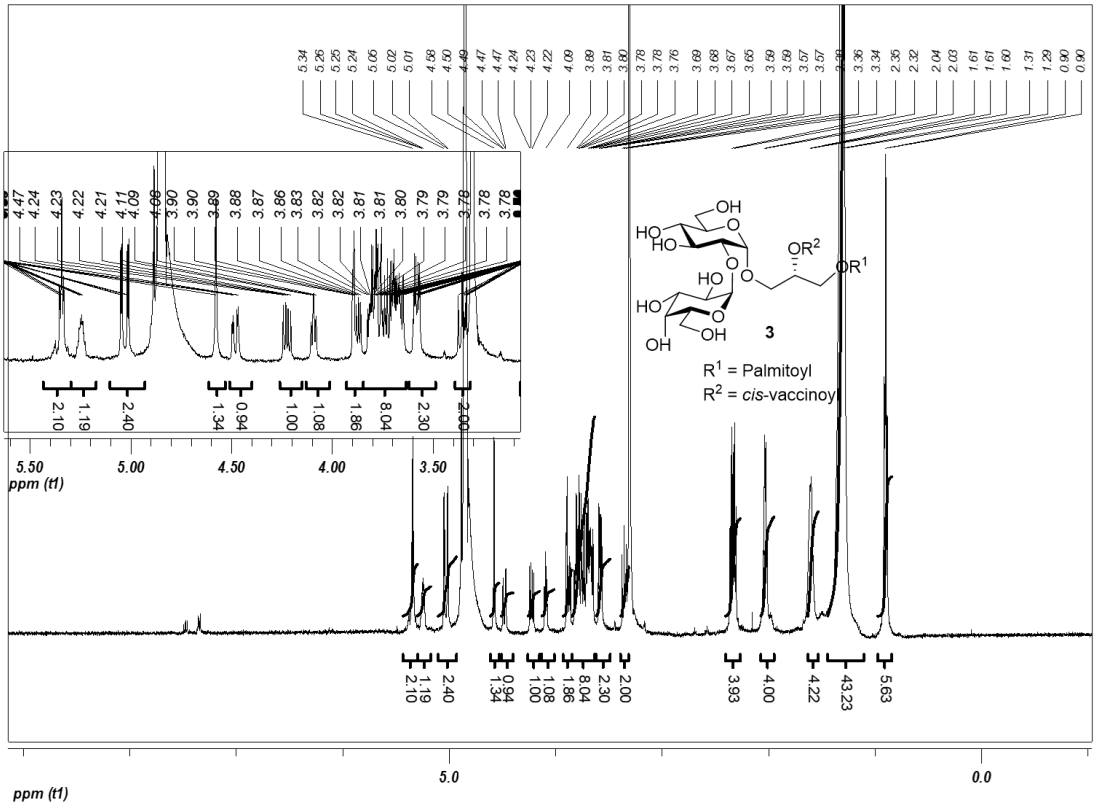

Figure S7. ^{1}H NMR (500MHz, MeOD) of compound **3**.

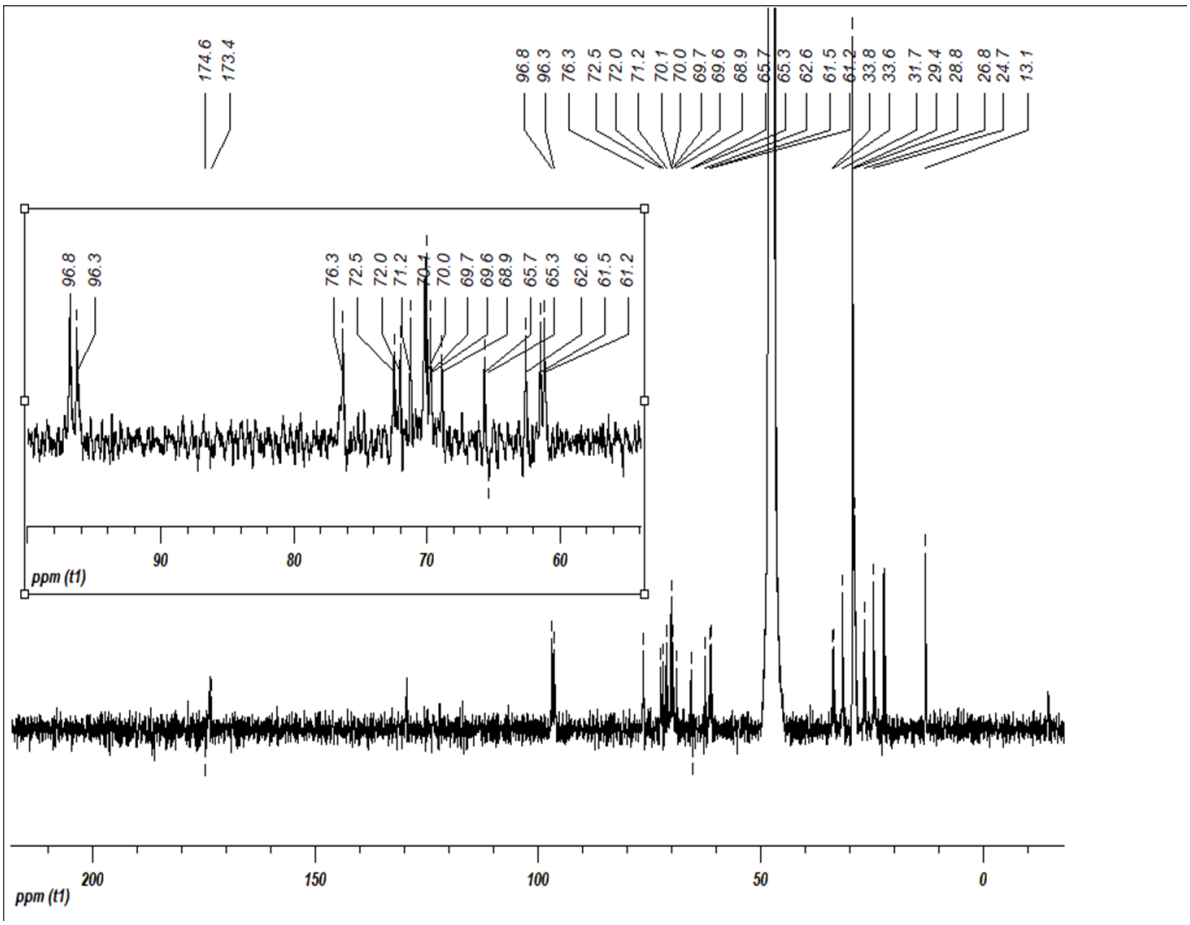

Figure S8. ^{13}C NMR (125MHz, MeOD) of compound **3**

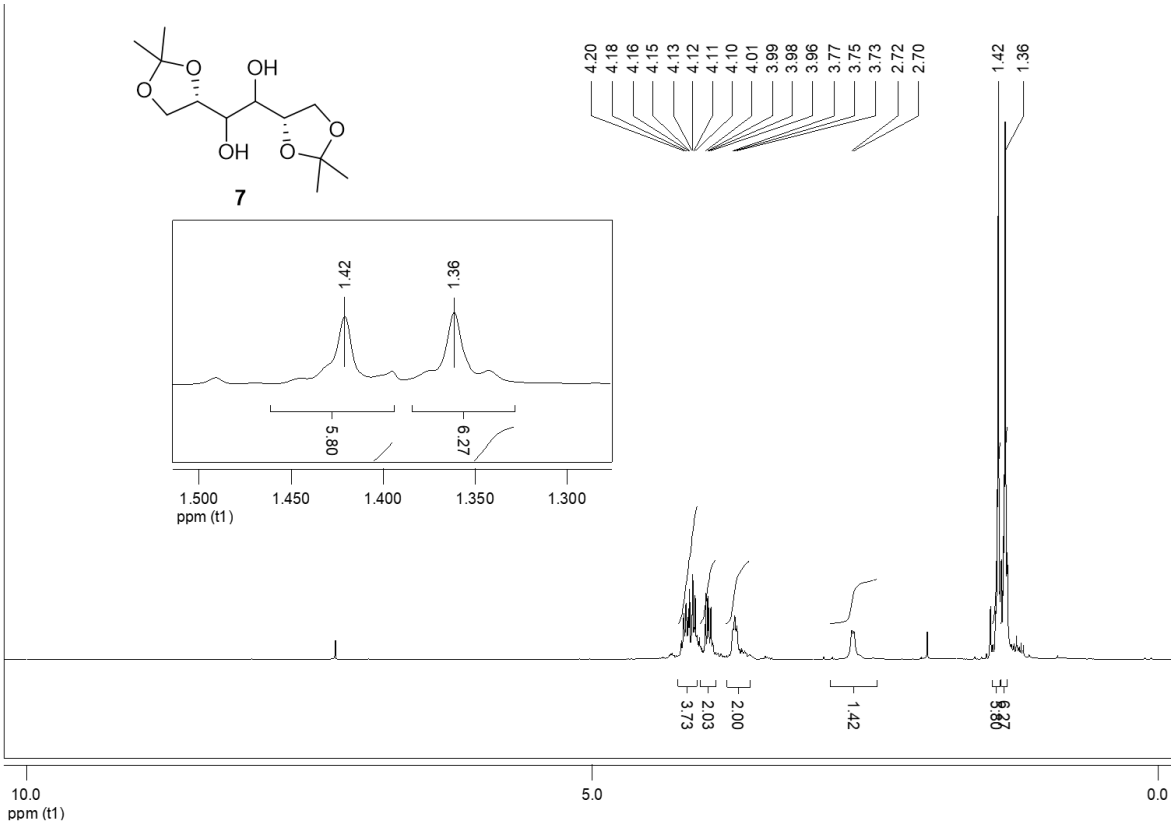

Figure S9. ^{1}H NMR (300MHz, $CDCl_3$) of compound **7.**

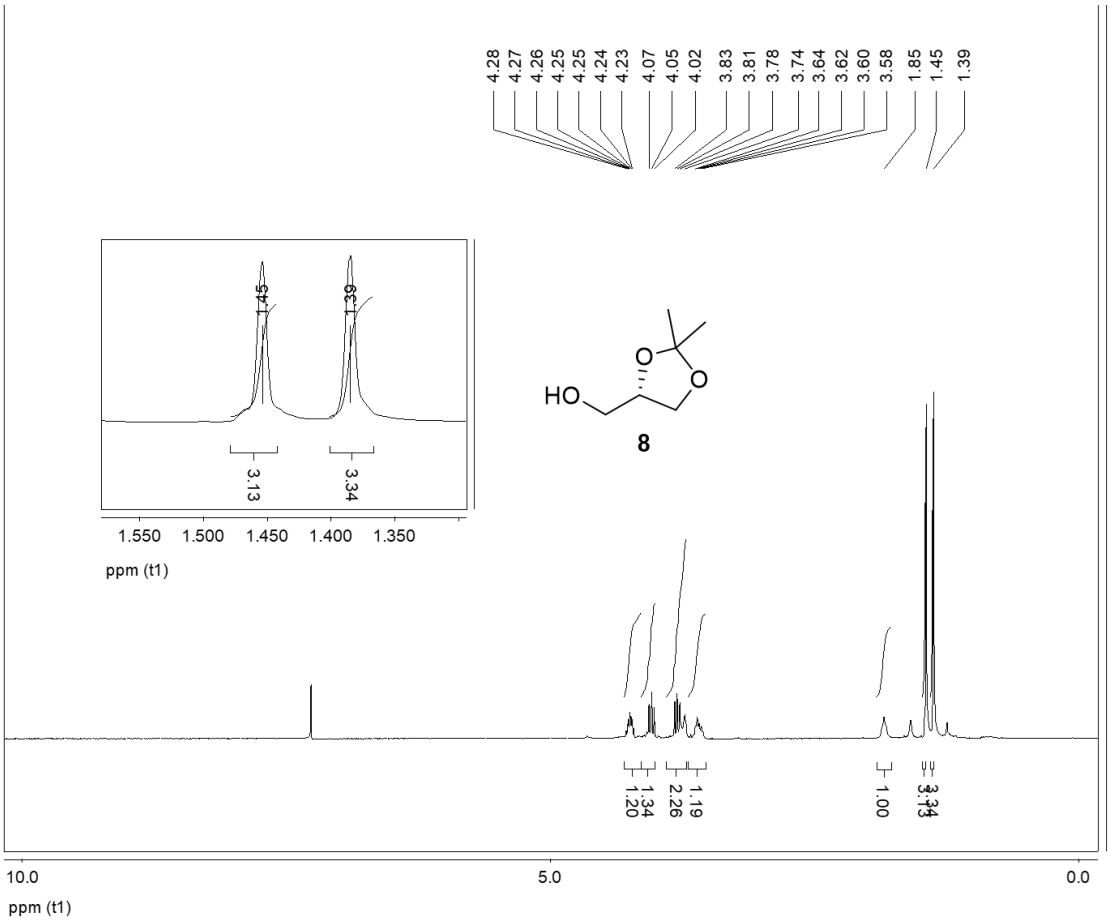

Figure S10. ^{1}H NMR (300MHz, $CDCl_3$) of compound **8**

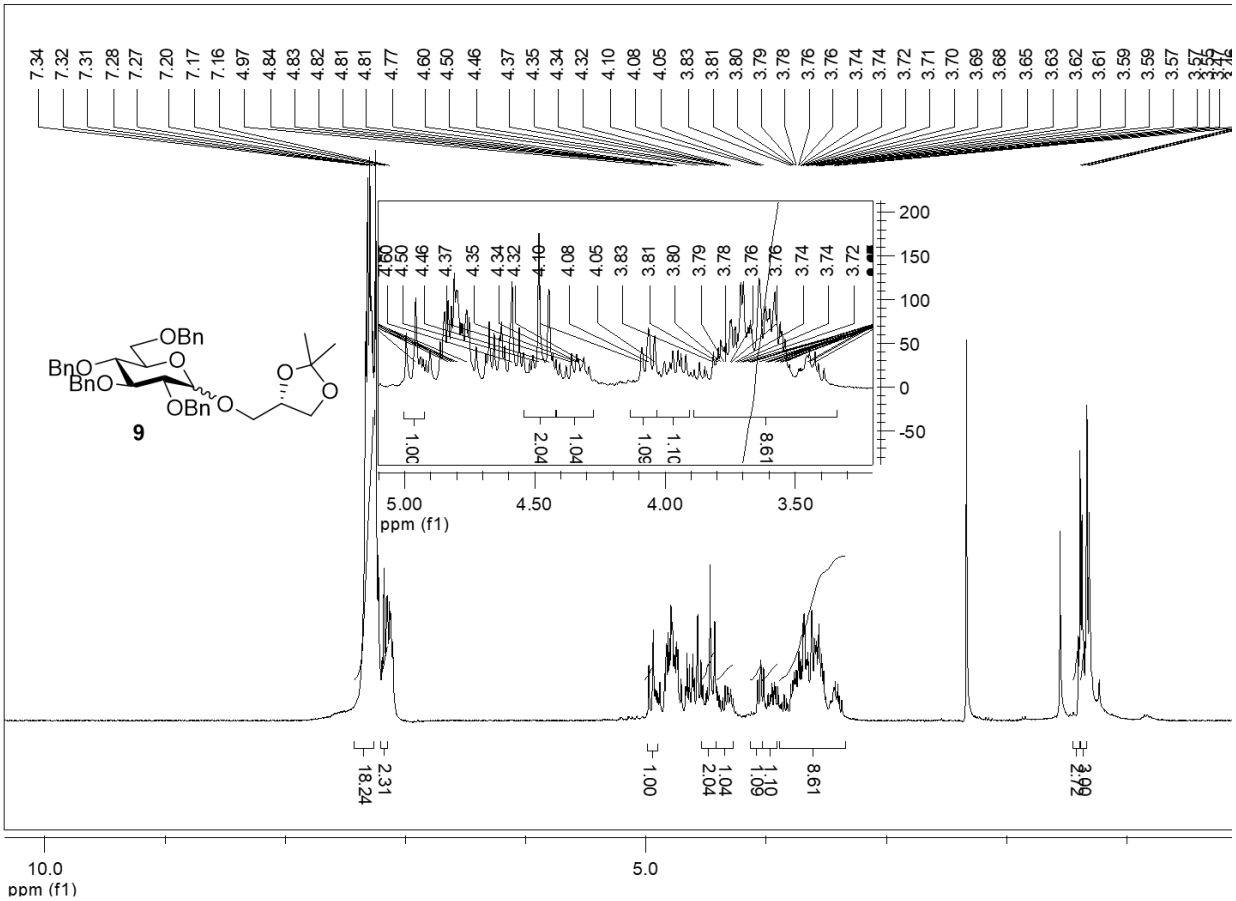

Figure S11. ^{1}H NMR (300MHz, $CDCl_3$) of compound **9**

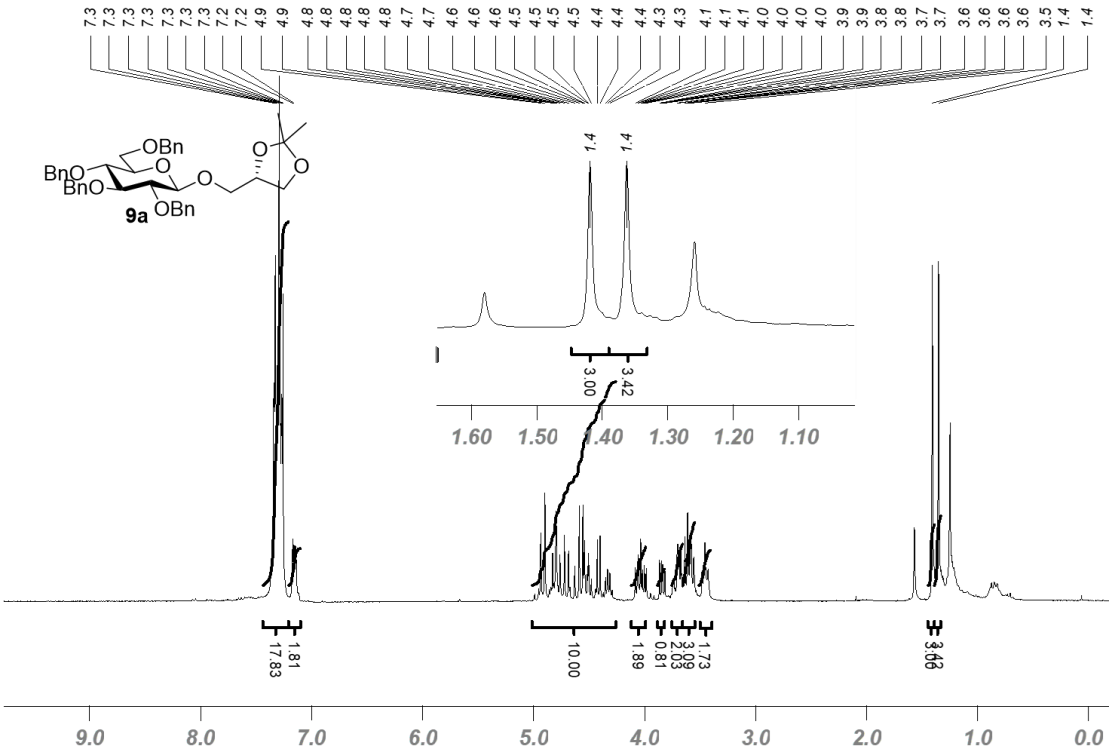

Figure S12. ^{1}H NMR (300MHz, $CDCl_3$) of compound **9a**

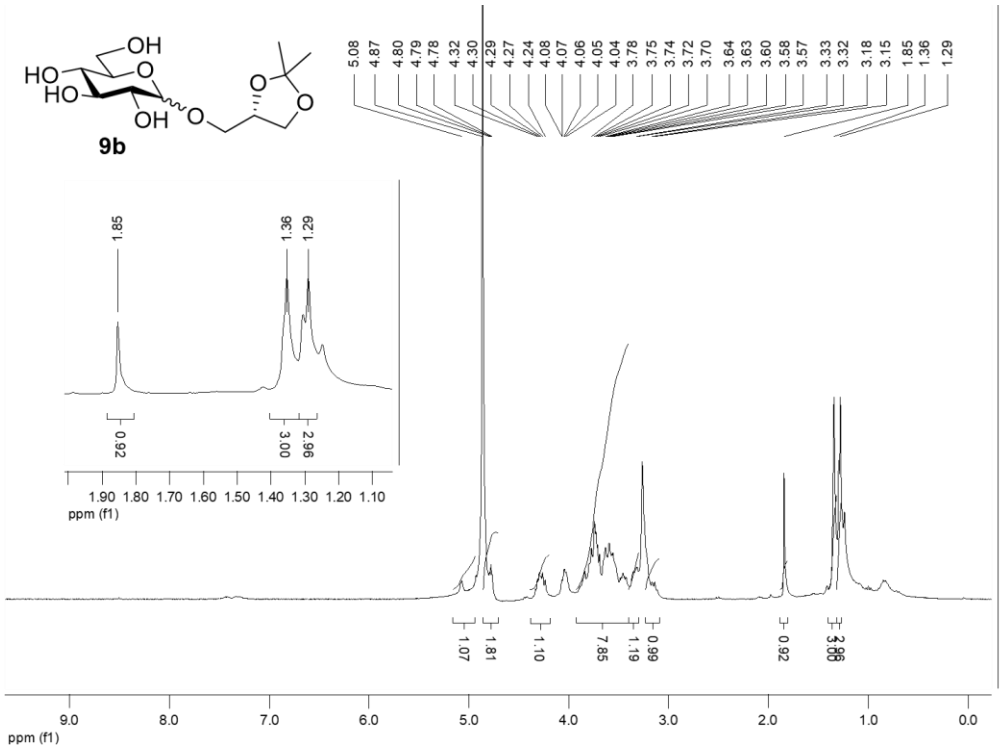

Figure S13. ^{1}H NMR (300MHz, MeOD) of compound **9b**

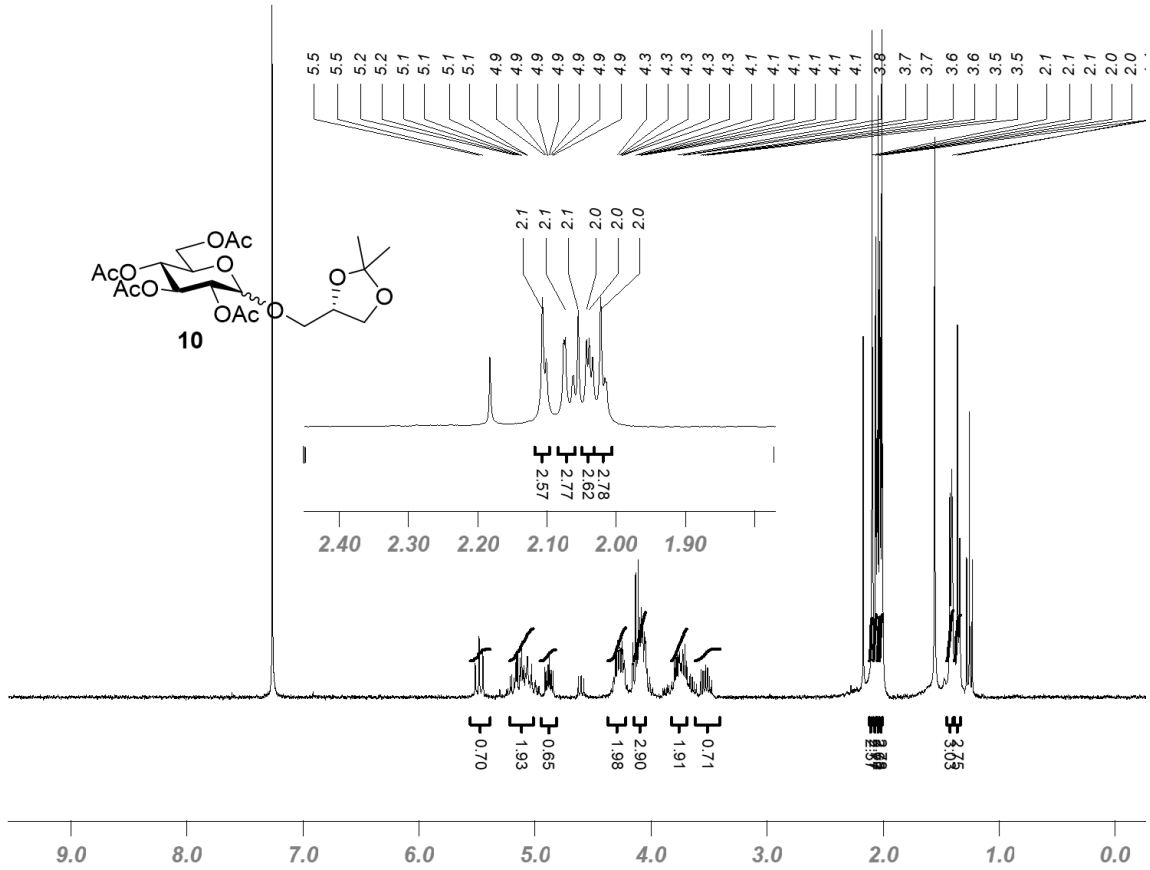

Figure S14. ^{1}H NMR (300MHz, $CDCl_3$) of compound **10**

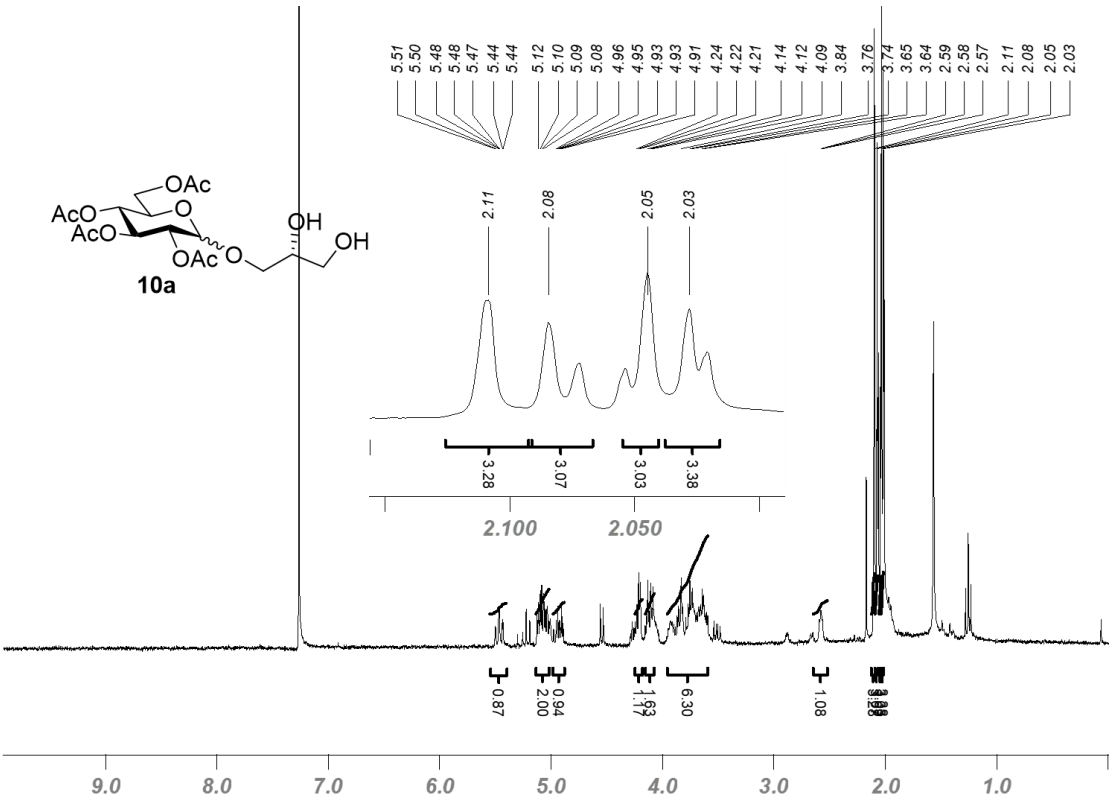

Figure S15. ^{1}H NMR (300MHz, $CDCl_3$) of compound **10a**

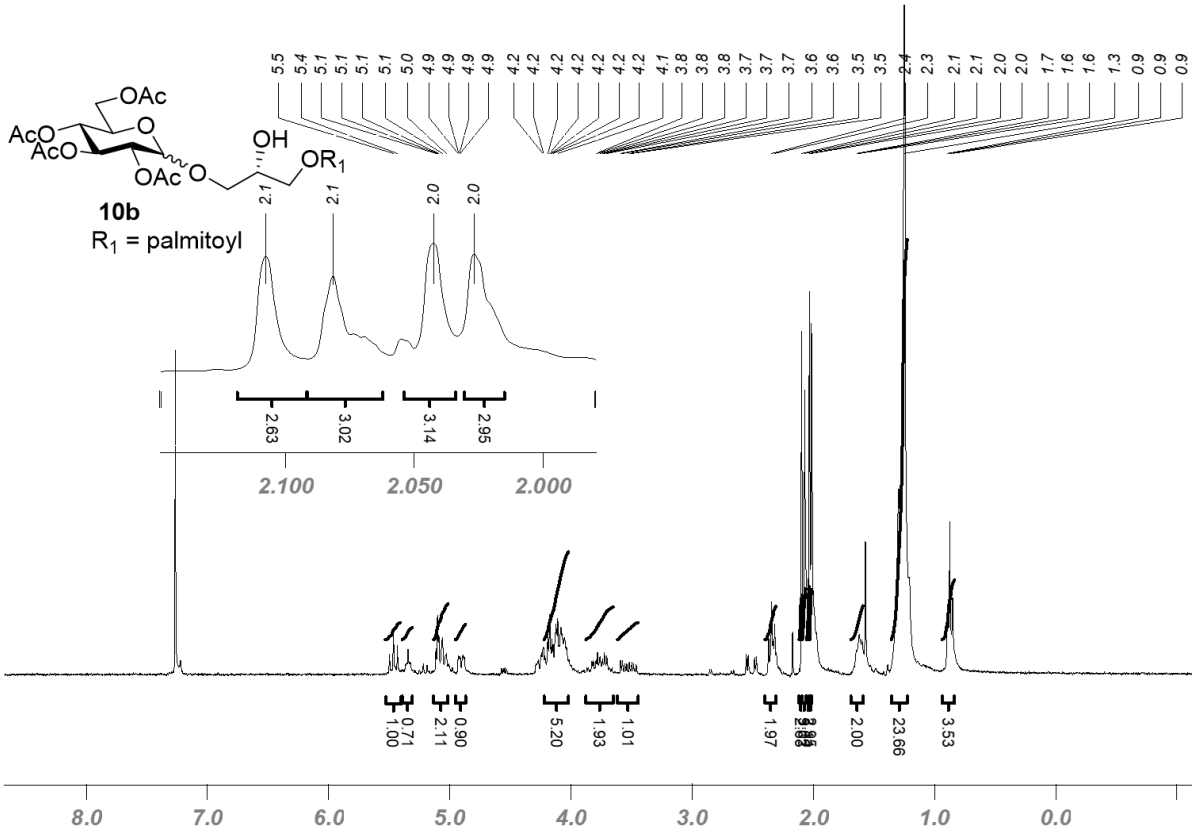

Figure S16. ^{1}H NMR (300MHz, $CDCl_3$) of compound **10b**

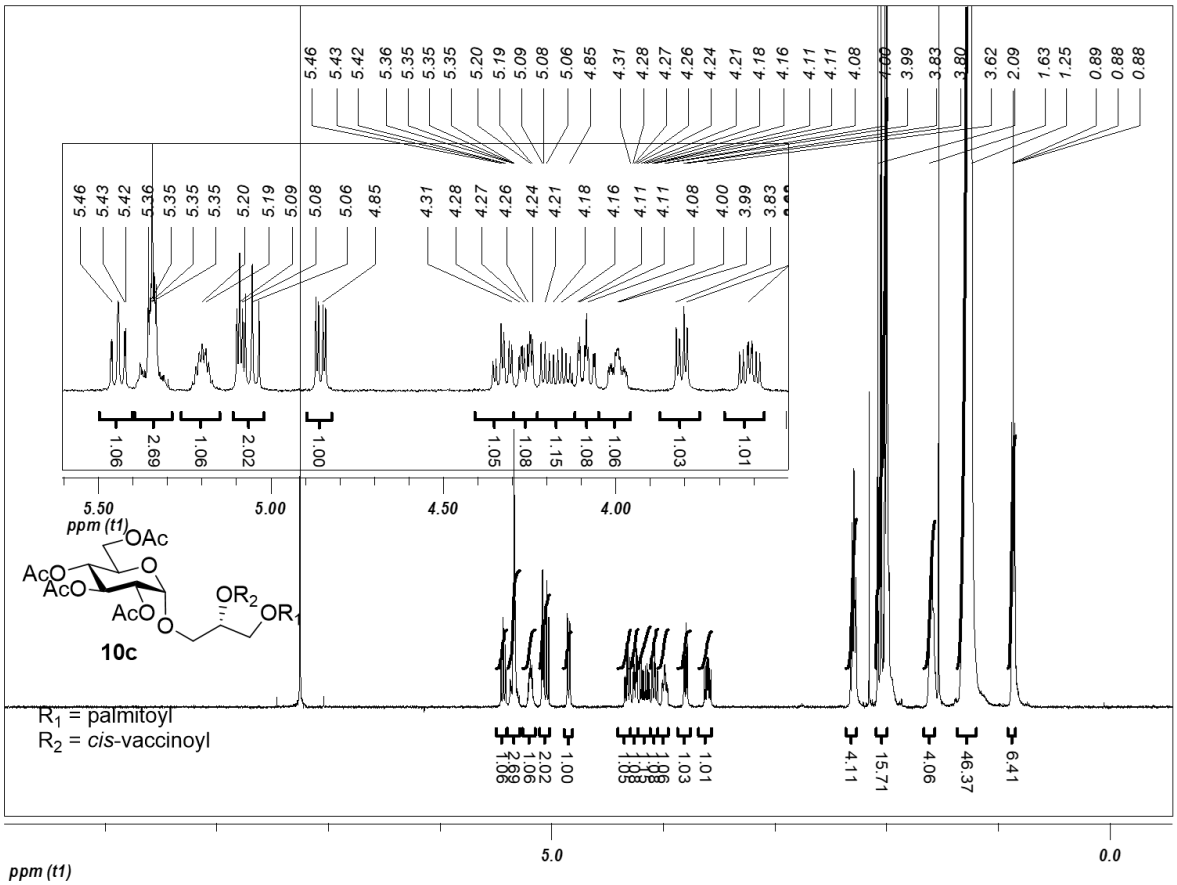

Figure S17. ^{1}H NMR (300MHz, $CDCl_3$) of compound **10c**

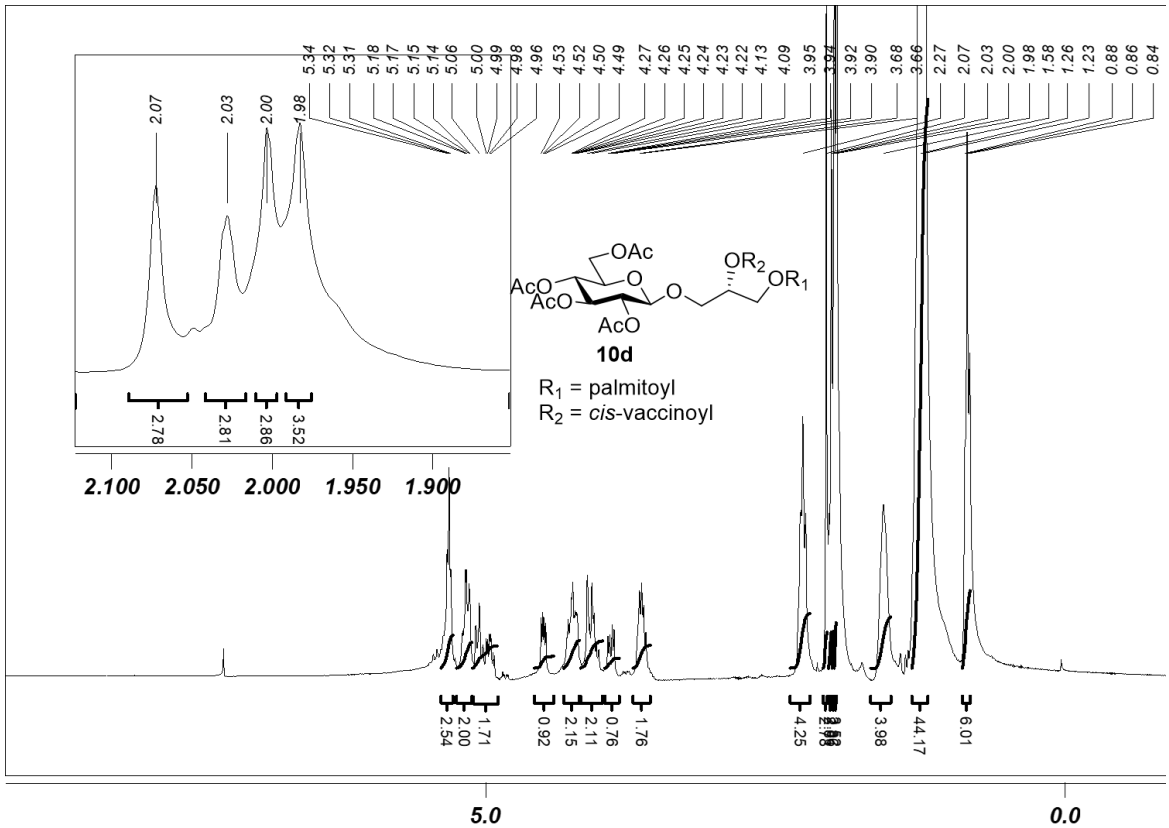

Figure S18. ^{1}H NMR (300MHz, $CDCl_3$) of compound **10d**

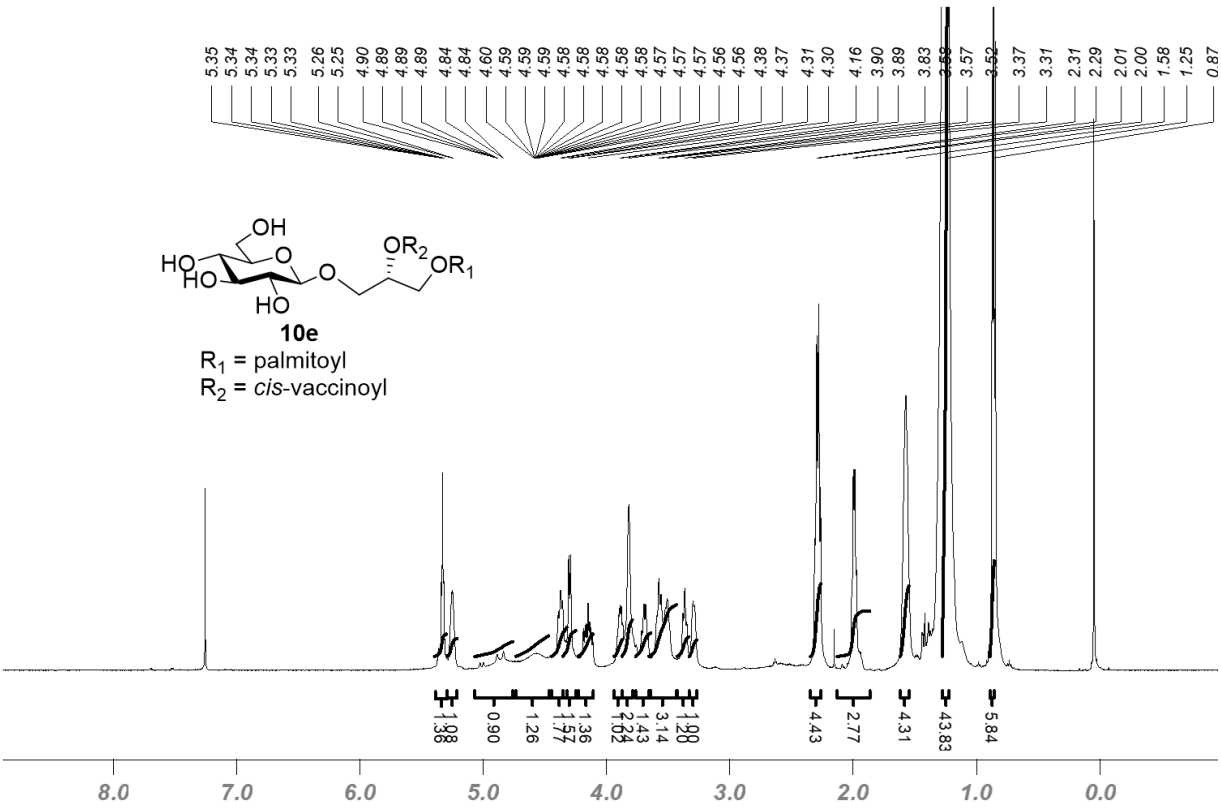

Figure S19. ^{1}H NMR (300MHz, $CDCl_3$) of compound **10e**

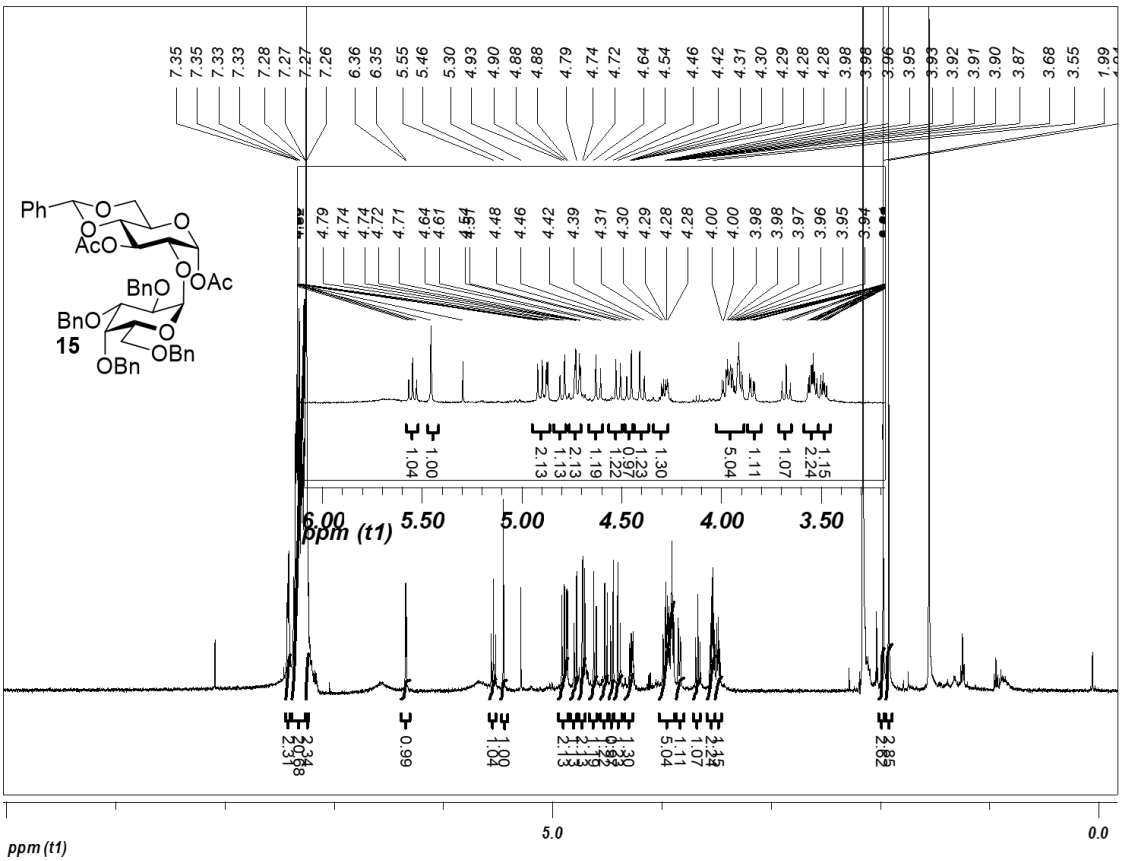

Figure S20. ^{1}H NMR (500MHz, $CDCl_3$) of compound **15**

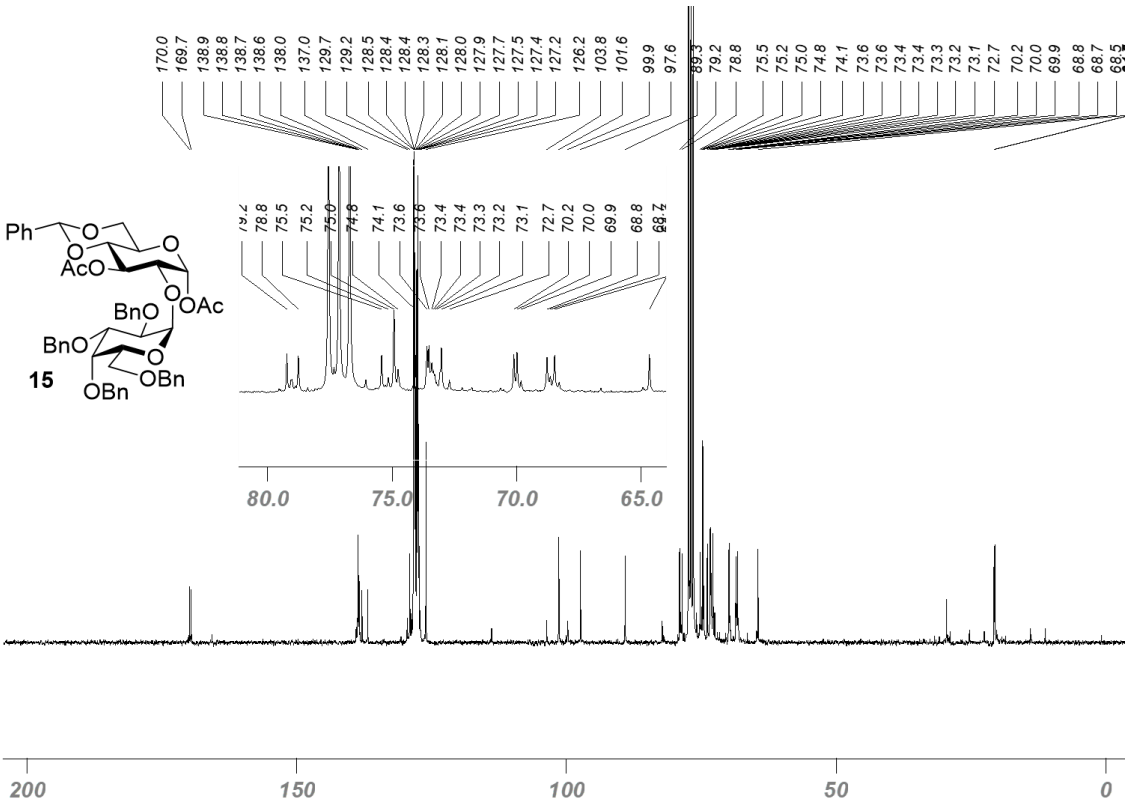

Figure S21. ^{13}C NMR (125MHz, $CDCl_3$) of compound **15**.

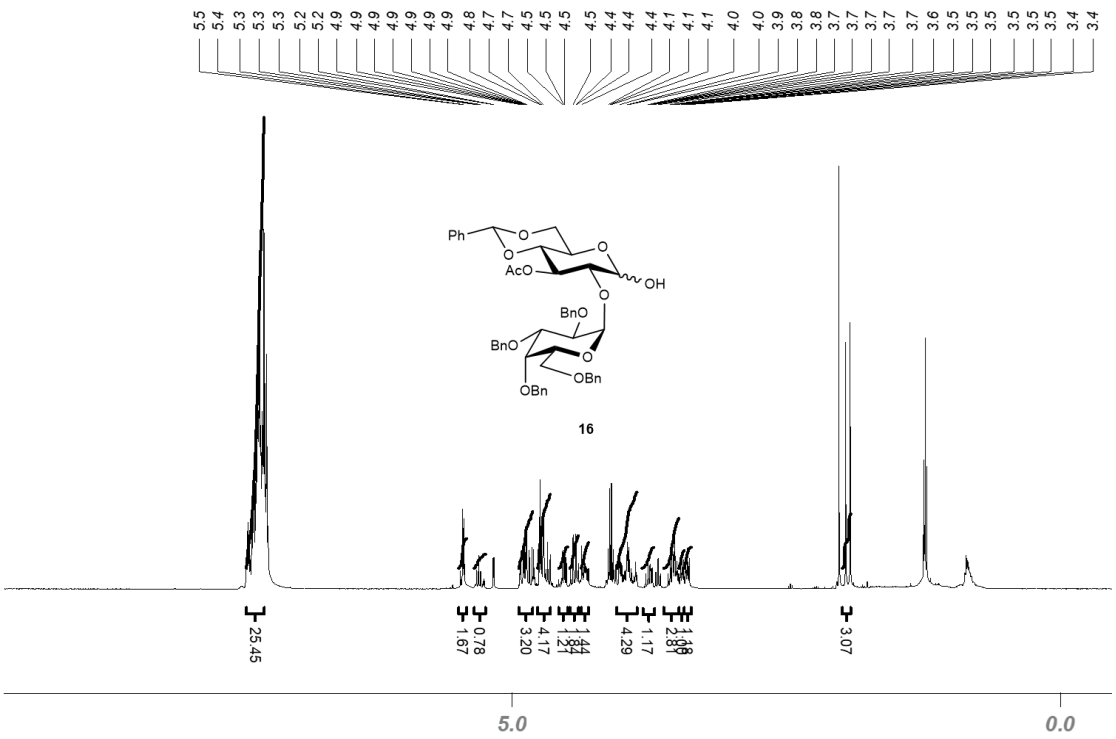

Figure S22. ^{1}H NMR (500MHz, $CDCl_3$) of compound **16.**

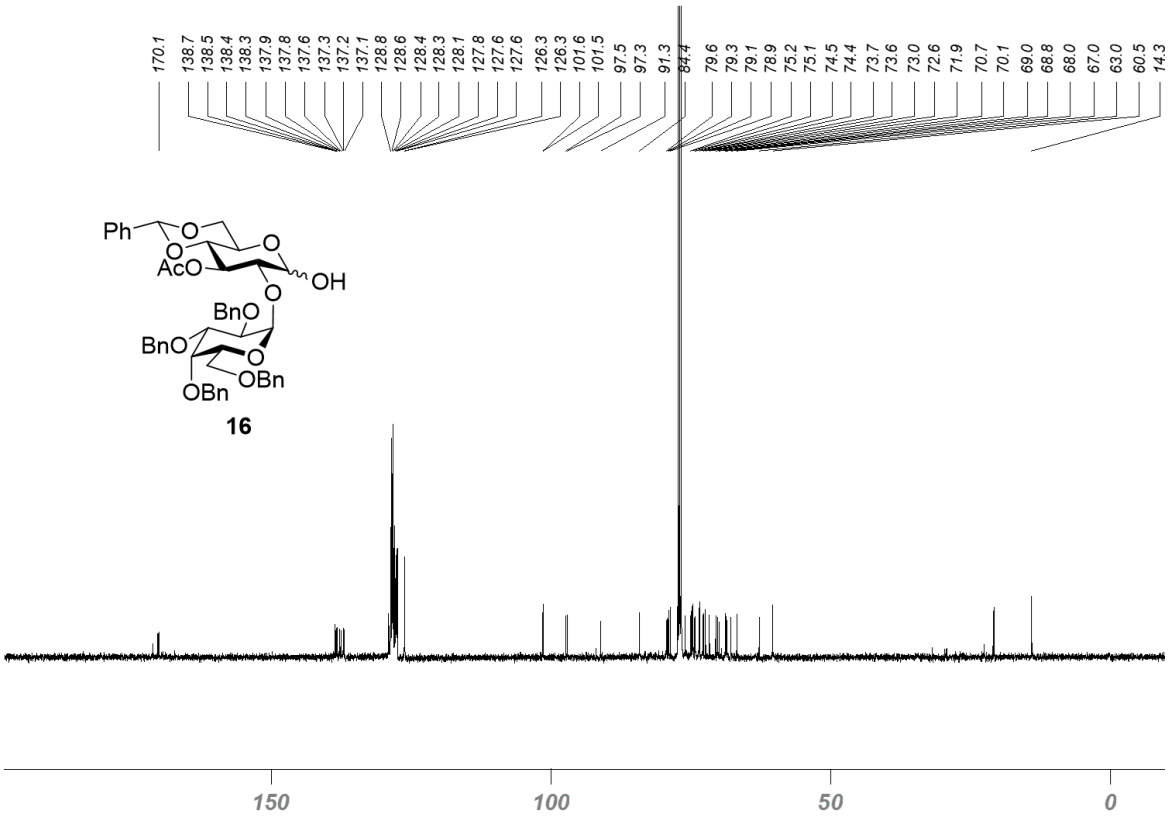

Figure S23. ^{13}C NMR (125MHz, $CDCl_3$) of compound **16**.

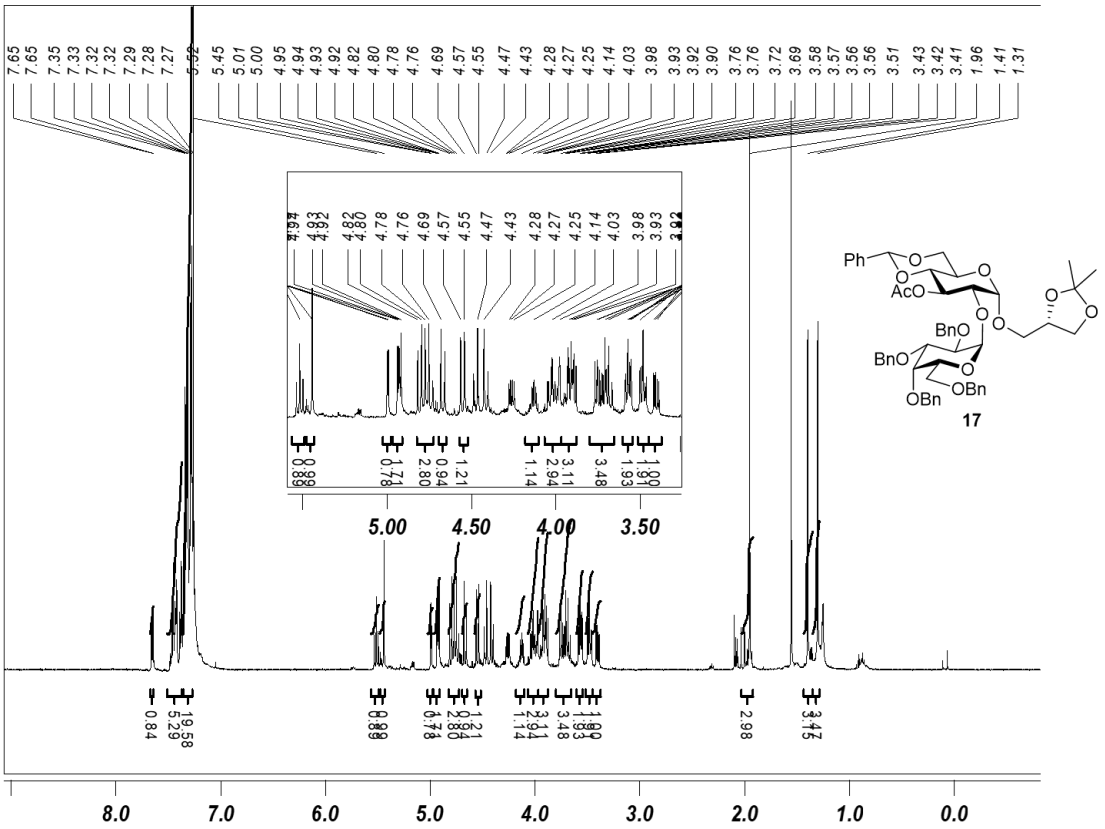

Figure S24. ^{1}H NMR (500MHz, $CDCl_3$) of compound **17.**

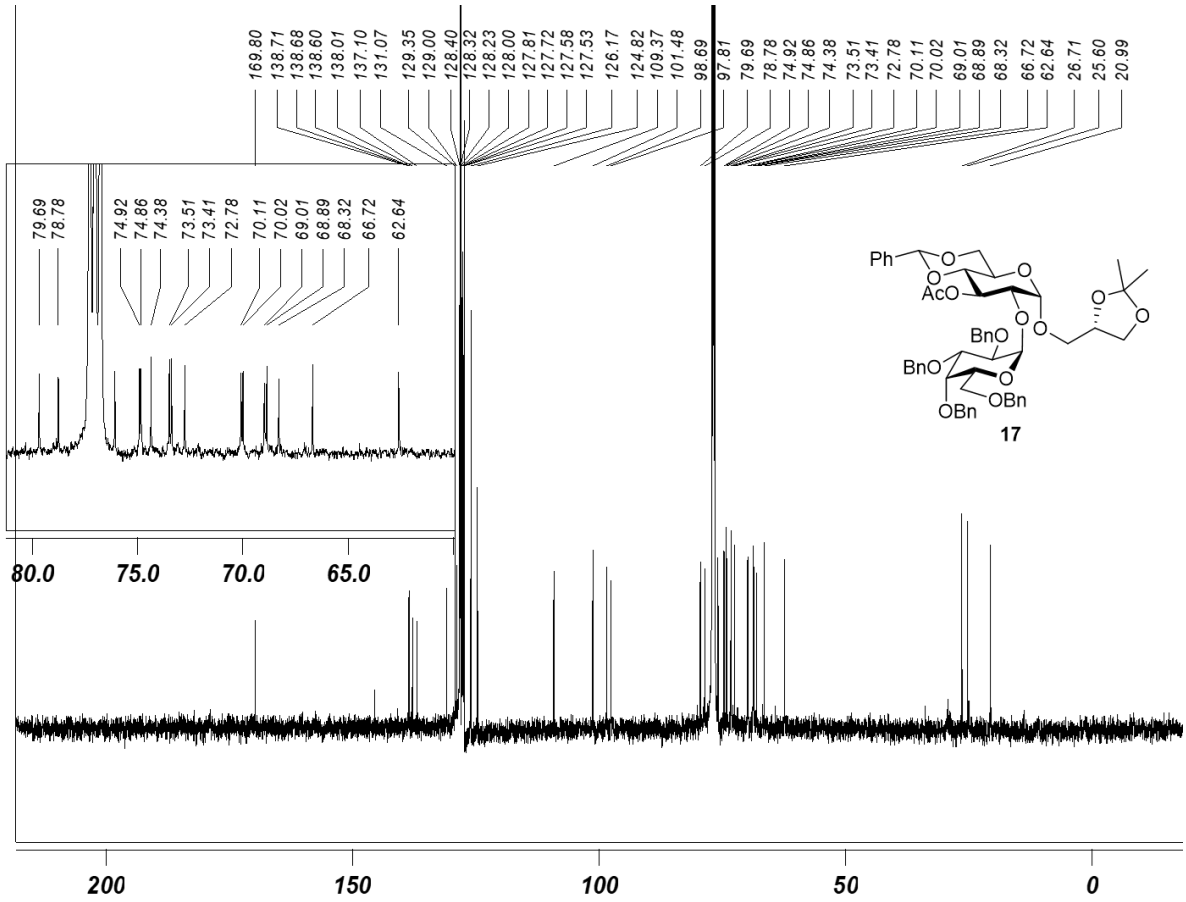

Figure S25. ^{13}C NMR (125MHz, $CDCl_3$) of compound **17**.

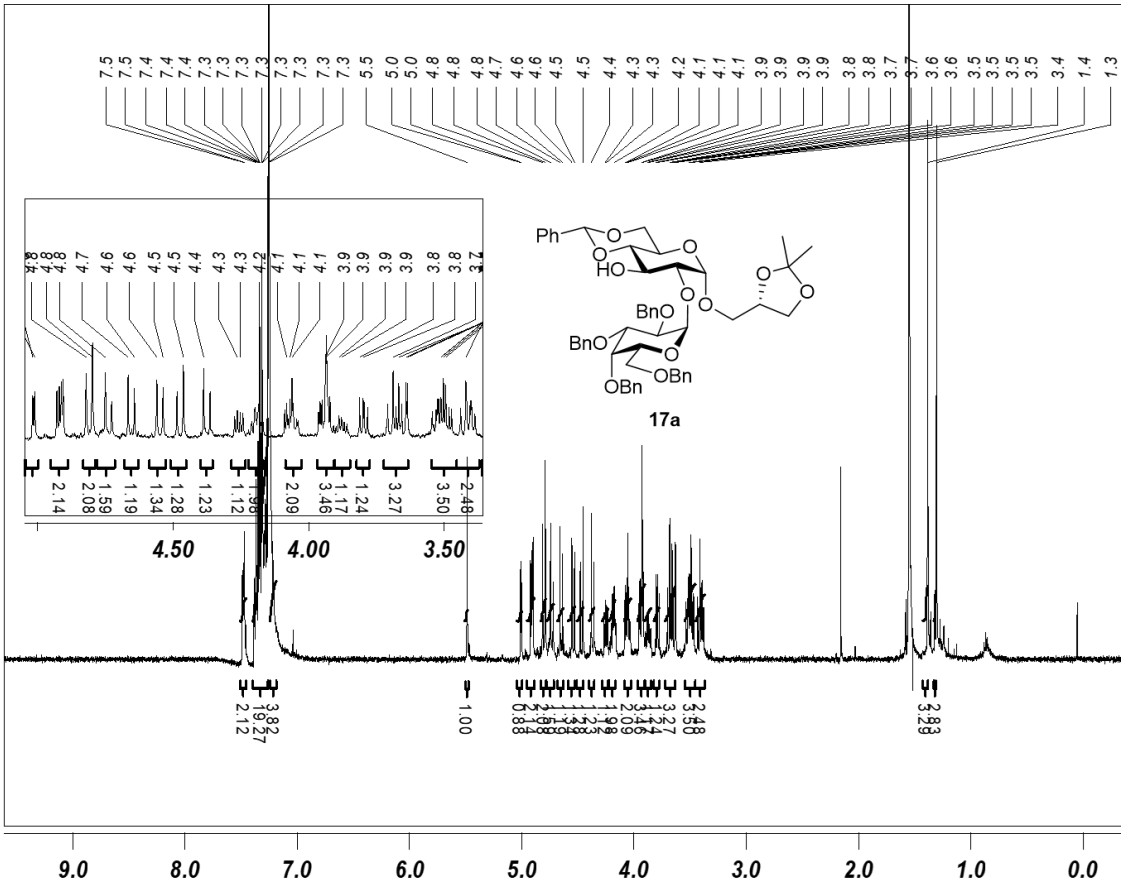

Figure S26. ^{1}H NMR (500MHz, $CDCl_3$) of compound **17a.**

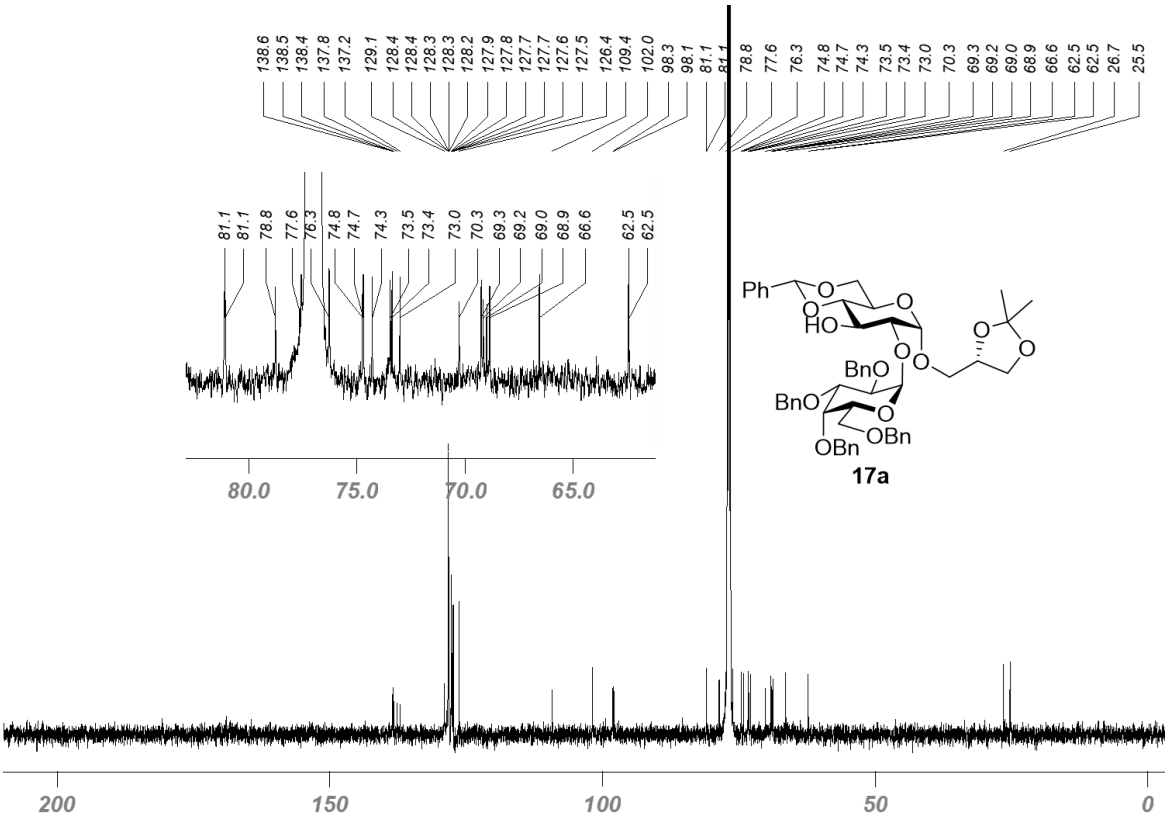

Figure S27. ^{13}C NMR (125MHz, $CDCl_3$) of compound **17a**.

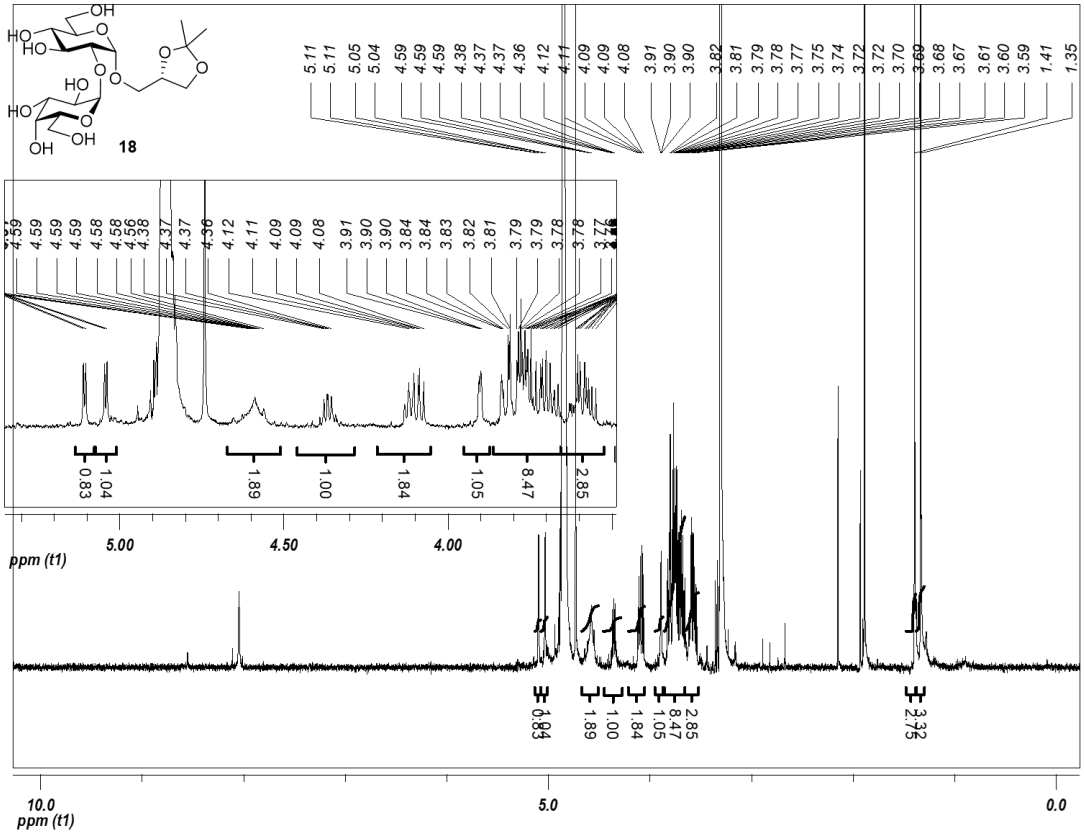

Figure S28. ^{1}H NMR (500MHz, MeOD) of compound **18.**

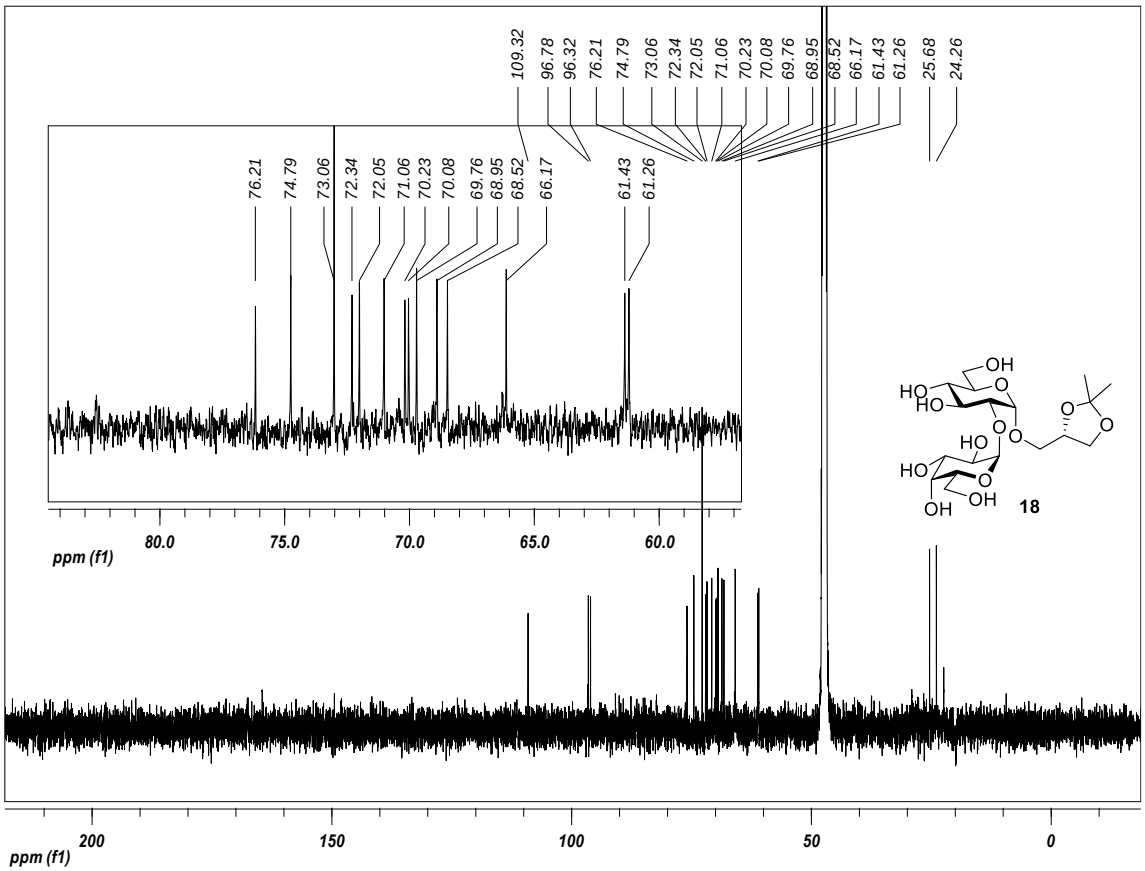

Figure S29. ^{13}C NMR (125MHz, MeOD) of compound **18**.

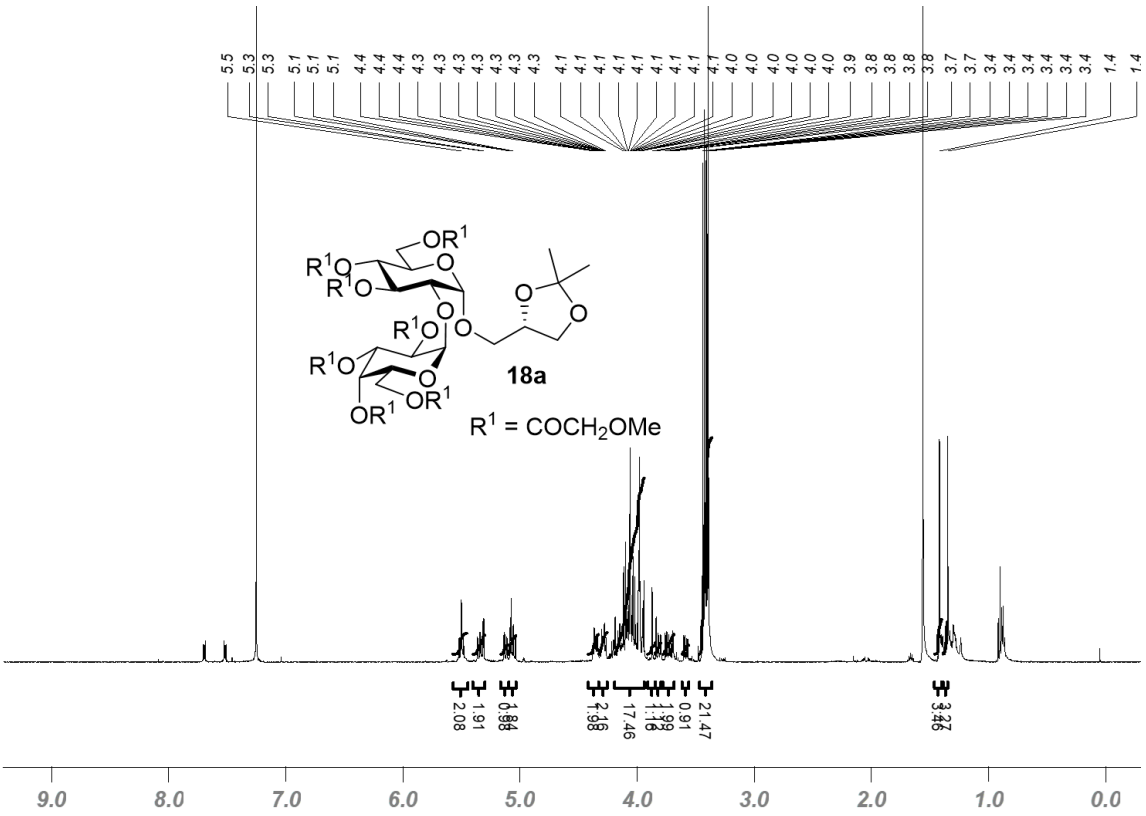

Figure S30. ^{1}H NMR (500MHz, MeOD) of compound **18a.**

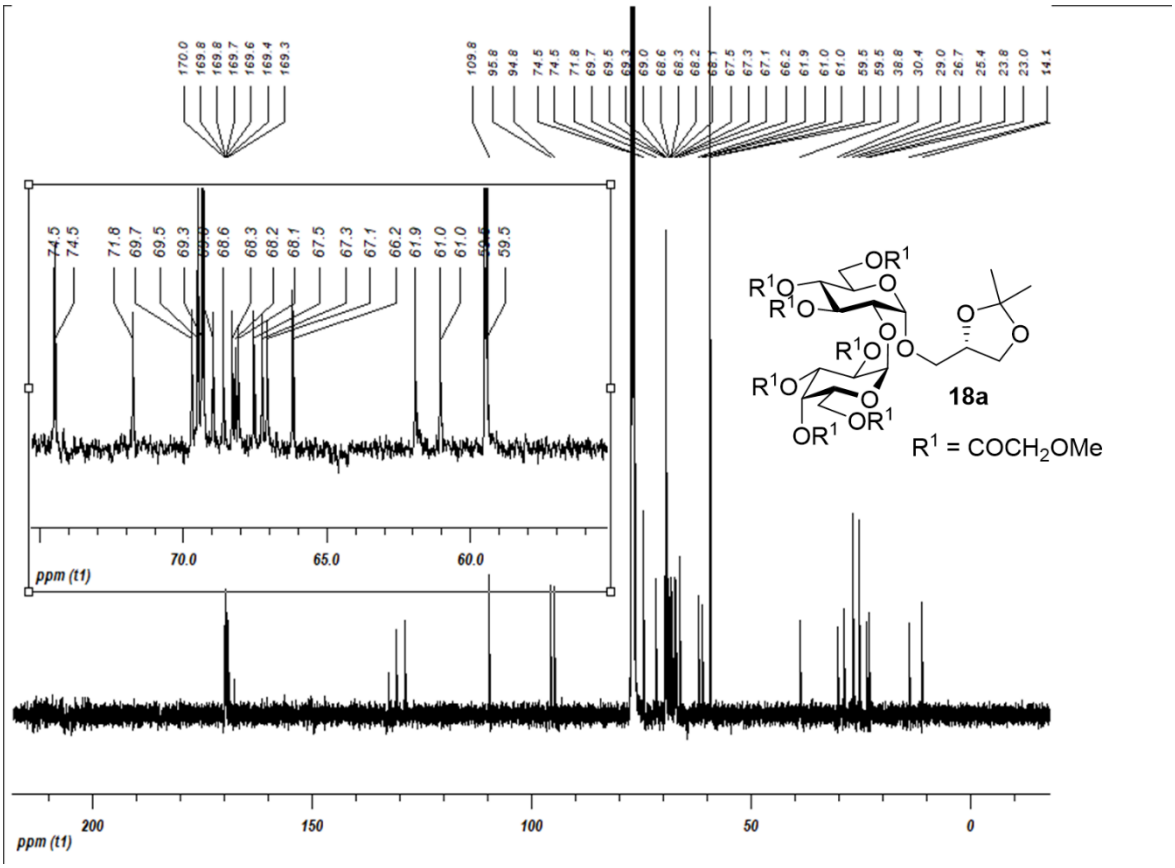

Figure S31. ^{13}C NMR (125MHz, MeOD) of compound **18a**.

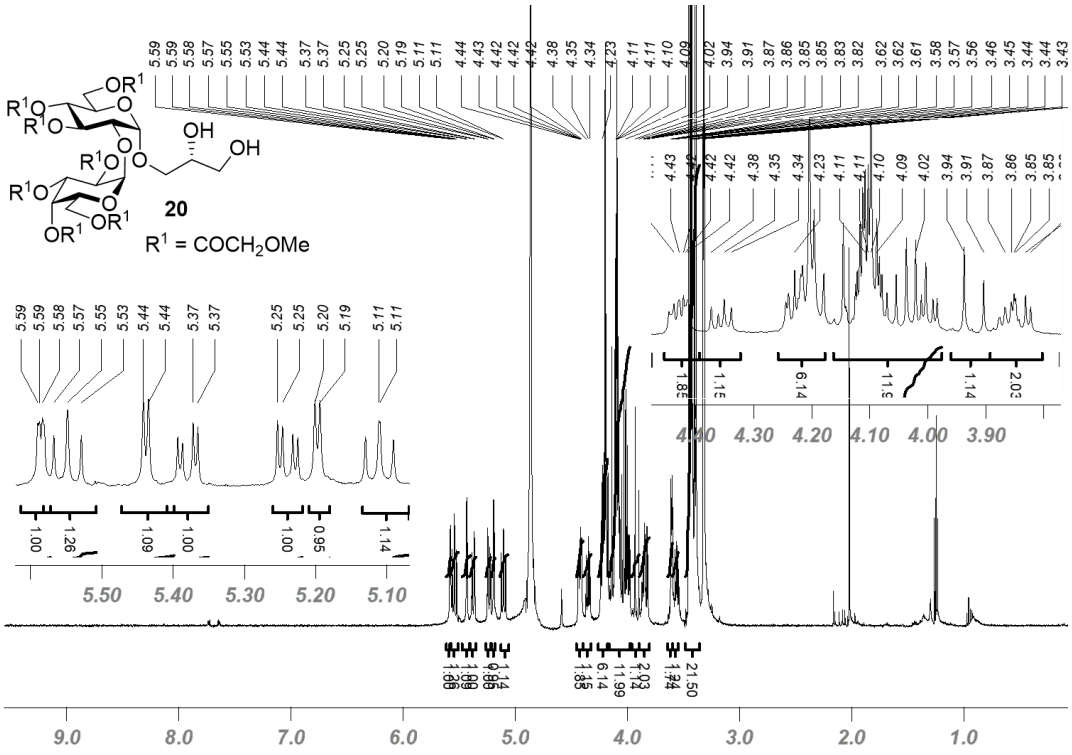

Figure S32. ^{1}H NMR (500MHz, MeOD) of compound **20.**

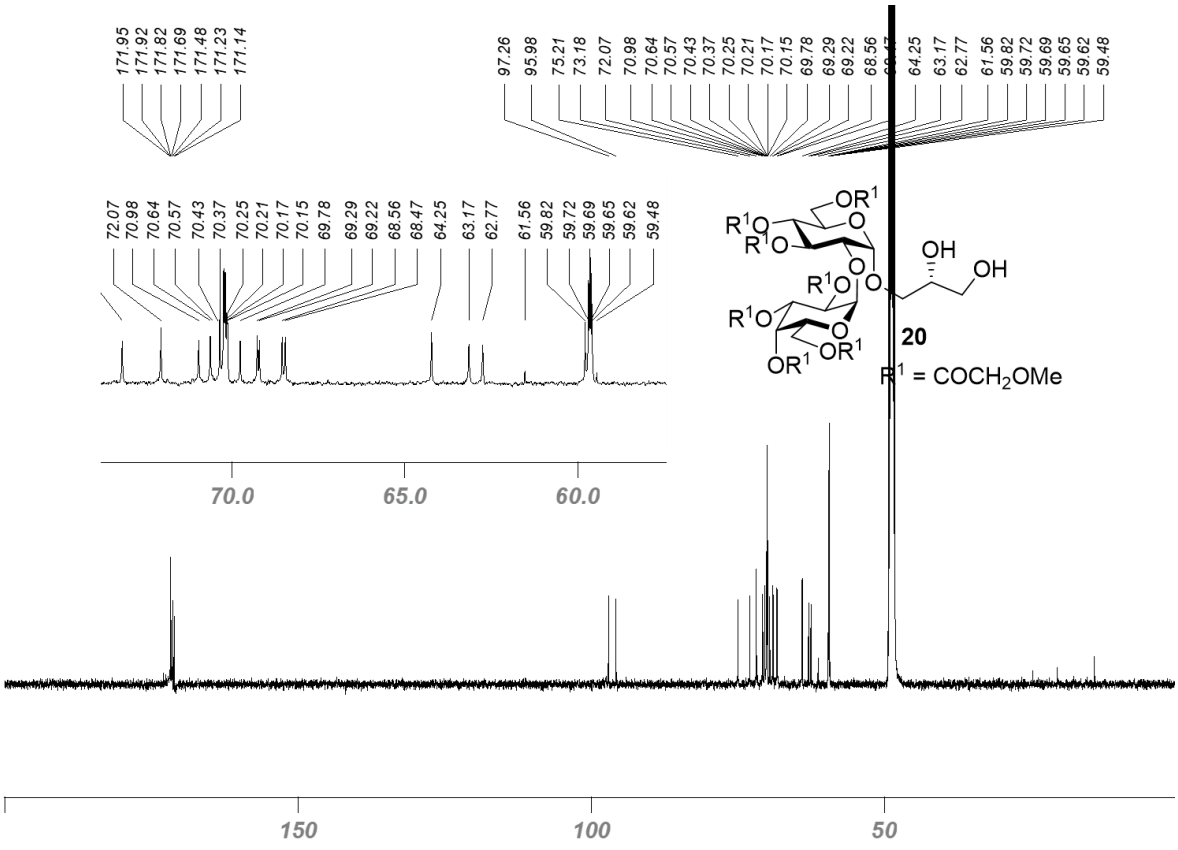

Figure S33. ^{13}C NMR (125MHz, MeOD) of compound **20**.

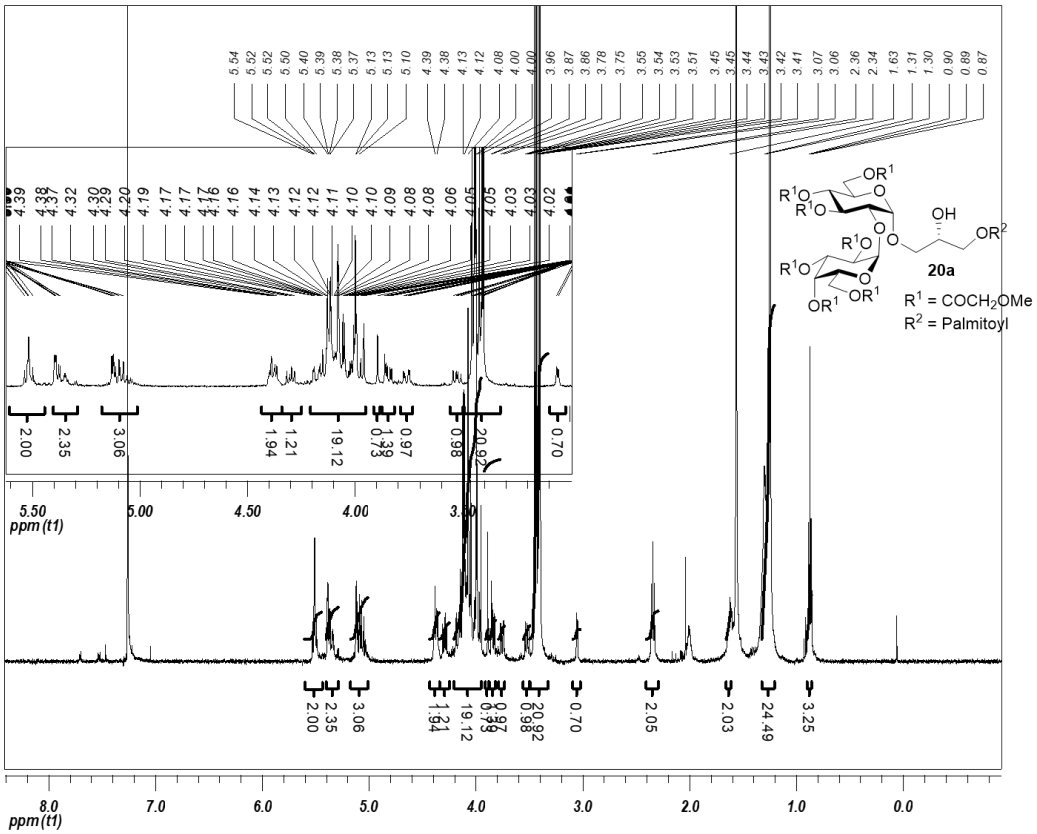

Figure S34. ^{1}H NMR (500MHz, $CDCl_3$) of compound **20a.**

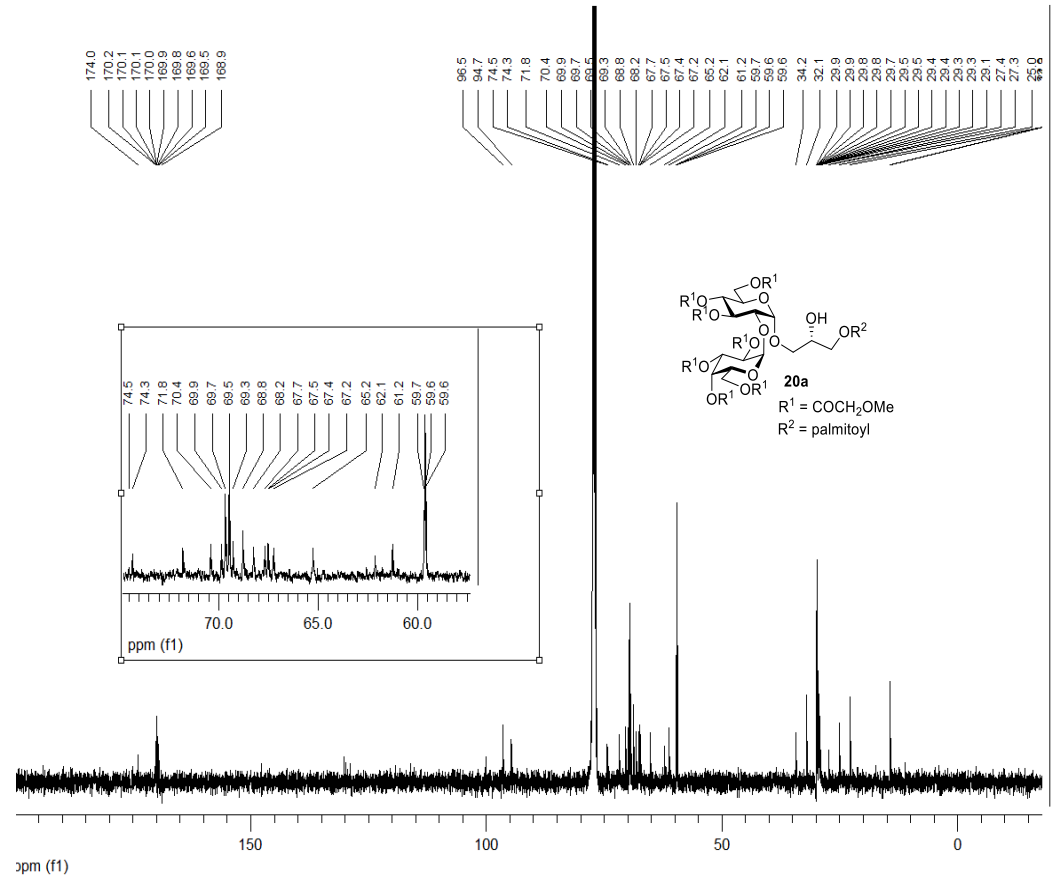

Figure S35. ^{13}C NMR (125MHz, $CDCl_3$) of compound **20a**.

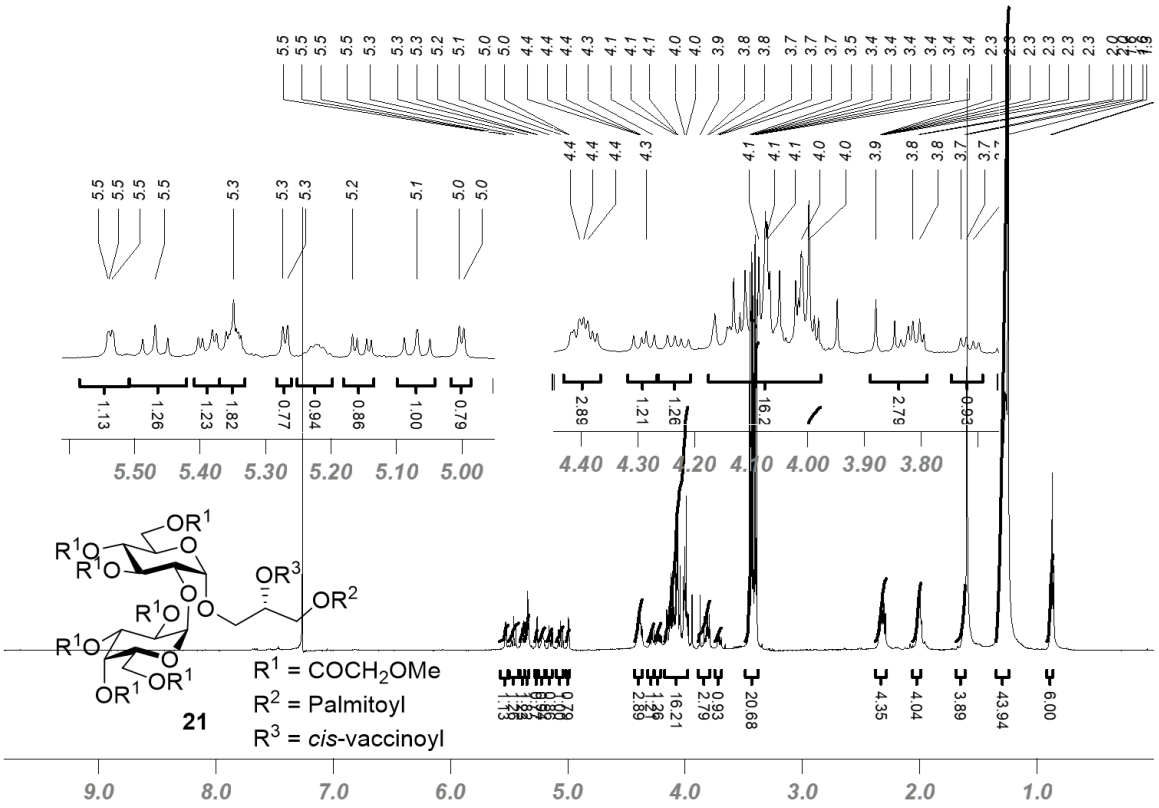

Figure S36. ^{1}H NMR (500MHz, $CDCl_3$) of compound **21.**

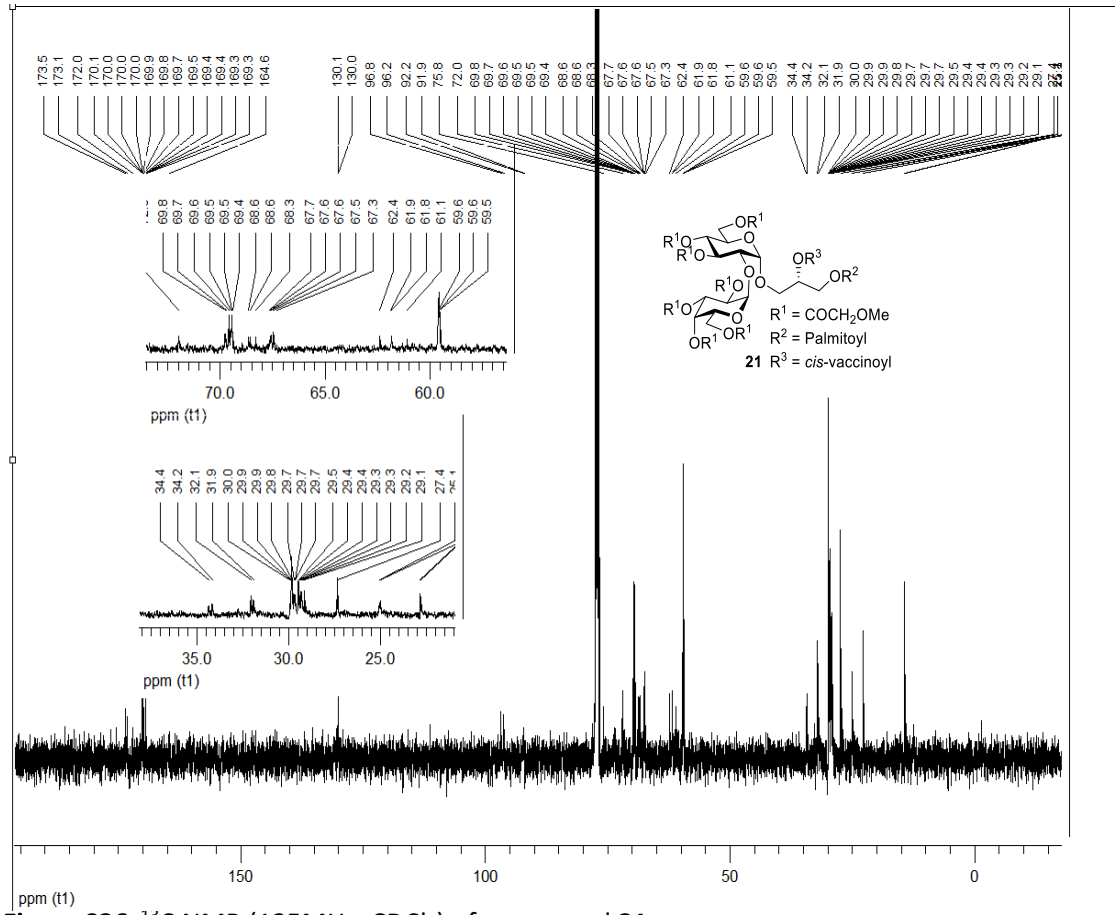

Figure S36. ^{13}C NMR (125MHz, $CDCl_3$) of compound **21**.

Reference

[1] Y. Kinjo, P. Illarionov, J. L. Vela, B. Pei, E. Girardi, X. Li, Y. Li, M. Imamura, Y. Kaneko, A. Okawara, Y. Miyazaki, A. Gomez-Velasco, P. Rogers, S. Dahesh, S. Uchiyama, A. Khurana, K. Kawahara, H. Yesilkaya, P. W. Andrew, C.-H. Wong, K. Kawakami, V. Nizet, G. S. Besra, M. Tsuji, D. M. Zajonc and M. Kronenberg, *Nat. Immunol.* **2011**, *12*, 966-974.